Willenbring, J. K., von Blanckenburg, F. (2010): Meteoric cosmogenic Beryllium-10 adsorbed to river sediment and soil: applications for Earth-surface dynamics. - Earth-Science Reviews, 98, 1-2, 105-122

DOI: 10.1016/j.earscirev.2009.10.008

Meteoric cosmogenic Beryllium-10 adsorbed to river sediment and soil: applications for Earth-surface dynamics

Earth-Science Reviews (2009), *doi:10.1016/j.earscirev.2009.10.008*

Jane K. Willenbring & Friedhelm von Blanckenburg

GFZ German Research Center for Geosciences
Telegrafenberg
14473 Potsdam, German

jane@gfz-potsdam.de Tel: +49-331-288-28600
fvb@gfz-potsdam.de Tel: +49-331-288-2850

Keywords: cosmogenic, meteoric, Beryllium, denudation, sediment, erosion, geomorphology

ABSTRACT

Rainfall scavenges meteoric cosmogenic ^{10}Be from the atmosphere. ^{10}Be falls to the Earth surface, where it binds tightly to sediment particles in non-acidic soils over the life-span of those soils. As such, meteoric ^{10}Be has the potential to be an excellent geochemical tracer of erosion and stability of surfaces in a diverse range of natural settings. Meteoric ^{10}Be has great potential as a recorder of first-order erosion rates and soil residence times. Even though this tracer was first developed in the late 1980s and showed great promise as a geomorphic tool, it was sidelined in the past two decades with the rise of the "sister nuclide", *in situ* ^{10}Be, which is produced at a known rate inside quartz minerals. Since these early days, substantial progress has been made in several areas that now shed new light on the applicability of the meteoric variety of this cosmogenic nuclide. Here, we revisit the potential of this tracer and we summarize the progress: (1) the atmospheric production and fallout is now described by numeric models, and agrees with present-day measurements and paleo-archives such as from rain and ice cores; (2) short-term fluctuations in solar modulation of cosmic rays or in the delivery of ^{10}Be are averaged-out over the time scale soils accumulate; (3) in many cases, the delivery of ^{10}Be is not dependent on the amount of precipitation; (4) we explore where ^{10}Be is retained in soils and sediment; (5) we suggest a law to account for the strong grain size dependence that controls adsorption and the measured nuclide concentrations; and (6) we present a set of algebraic expressions that allows calculation of both soil or sediment ages and erosion rates from the inventory of meteoric ^{10}Be distributed through a vertical soil column. The mathematical description is greatly simplified if the accumulation of ^{10}Be is at steady state with its export through erosion. In this case, a surface sample allows for the calculation of an erosion rate. Explored further, this approach allows calculation of catchment-wide erosion rates from river sediment, similar to the approach using ^{10}Be produced *in situ*. In contrast to the *in situ* ^{10}Be approach, however, these analyses can be performed on any sample of fine-grained material, even where no quartz minerals are present. Therefore, this technique may serve as a tool to date sediment where no other chronometer is available, to track particle sources and to measure Earth-surface process rates in soil, suspended river sediment, and fine-grained sedimentary deposits.

1. INTRODUCTION

The radioactive cosmogenic isotope Beryllium-10 (^{10}Be) is produced via interactions of high energy cosmic radiation with target nuclei both in the atmosphere ('meteoric') and within mineral lattices in material at the Earth's surface ('*in situ*') (Fig. 1). Both *in situ*-produced and meteoric ^{10}Be accumulate in surficial deposits over time such that the concentration of the nuclide is related to both the age and stability of the surface material. Applications of ^{10}Be in the late 1980s and early 1990s in the study of terrestrial surface processes emphasized 'meteoric' ^{10}Be (good summaries are given by L. Brown, 1984; McHargue and Damon, 1991). Use of 'meteoric' ^{10}Be as a tool was developed to measure soil residence times (e.g. Pavich et al., 1986; Barg, 1992), trace soil transport (e.g. McKean et al., 1992), quantify river sediment and dissolved fluxes (e.g. L. Brown et al., 1988; You et al., 1988; E. Brown et al., 1992), seafloor sedimentation rates (e.g. Bourlès et al., 1989), determine growth rates of oceanic

Fe-Mn crusts (Segl et al., 1989), reconstruct the Earth's paleomagnetic field strength from deep-sea sediments and ice cores (Frank et al., 1997; Wagner et al., 2001), determine past solar activity from ice cores (Muscheler et al., 2000); explore metal scavenging processes in the oceans (Anderson et al., 1990); trace ocean currents (e.g. von Blanckenburg et al., 1996) and snow accumulation rate reconstruction (Wagner et al., 2001). In 1991, D. Lal published a ground-breaking paper on the use of *in situ*-produced cosmogenic nuclides, for which the physical rules of production were so well described that the attention of the Earth-surfacecommunity turned toward this new system. In the last decade or so, *in situ*-produced ^{10}Be has been used to quantitatively measure erosion rates on surfaces exposed to cosmic radiation (Nishiizumi et al., 1989) and for entire watersheds (Granger et al., 1996; Bierman and Steig, 1996, von Blanckenburg, 2005) and has been thoroughly exploited as a robust surface exposure dating technique over the span of the last 10^2-10^7 yr (Gosse and Phillips, 2001; Cockburn and Summerfield 2004).

However, *in situ*-produced ^{10}Be techniques have some analytical and technical difficulties that limit their applications. First, the analytical requirements (physical and chemical mineral purification, rare nuclide isolation and AMS analysis) are extreme from both from a time and cost perspective, and has precluded major large-scale efforts. Secondly, to date, one of the most useful techniques for answering landscape erosion questions (i.e. measurement of *in situ*-produced ^{10}Be) requires a large quantity of pure, coarse-grained quartz. These types of sediments are not reliably available in continuous sedimentary records (offshore depo-centers, lacustrine environments etc.) such that despite initial attempts, the reconstruction of past erosion rate histories (Granger and Muzikar, 2001; Schaller et al., 2002; Fuller et al., 2009) has still not been established in a routine manner.

In notably farsighted applications, L. Brown et al. (1988) and You et al. (1988) used meteoric ^{10}Be in river sediment as a quasi-quantitative proxy for watershed erosion rate. In this application, the authors assumed that the integrated delivery rate of ^{10}Be from the atmosphere equaled the flux of ^{10}Be out of the basin through sediment transport such that basin-scale mass loss rates can be calculated. The flux out of the basin was calculated by multiplying the sediment yield of the catchment with the concentration of meteoric ^{10}Be on these sediment samples. However, at any given time, the measured concentration of ^{10}Be in soil, river sediment, or in lake bottom sediments reflects a complex interplay among the production of nuclides in the atmosphere, the delivery of ^{10}Be to the surface through rain, dry-fallout, and dust, and as well as the retention of ^{10}Be in the substrate and its stability with regards to erosion. All these factors were more uncertain at the time of these 1988 publications. Additionally, the need for robust sediment yield measurements to normalize the outflux of ^{10}Be from a basin and the discrepant time scales of sediment yield measurements and the build-up of ^{10}Be in the soil also limited widespread application of the technique.

Advances have been made in the past yr in the form of better models and measurements of production, adsorption, redistribution and retention as well as the ability to compare *in situ* and atmospheric cosmogenic ^{10}Be. Our main objective in this paper is to use these advancements and to revisit some of the processes that change the concentrations of this long-lived nuclide, meteoric ^{10}Be, through time and through a soil profile and to reappraise its utility as a sediment tracer in a variety of settings. We will also re-evaluate the technique of L. Brown et al. (1988) to evaluate conditions and settings under which an adaptation of this technique could provide a useful new tool for quantifying long-term rates of erosion.

2. PRINCIPLES OF THE METEORIC ^{10}BE TRACER

Beryllium-10 (^{10}Be) is a very rare, radioactive nuclide that is not present in natural materials unless these are exposed to cosmic radiation (Lal, 1991). ^{10}Be and other nuclides (Beryllium-7, Carbon-14) are produced in the atmosphere when cosmic rays strike the Earth's atmosphere. They collide with and undergo nuclear reactions with the nuclei of nitrogen, oxygen, argon and the other atmospheric gases. Most of the cosmogenic nuclides are produced in spallation reactions. In a spallation reaction, a high energy neutron (or other nucleon) breaks-up a target nucleus to produce several lighter particles. After production, the particle-reactive ^{10}BeO or ^{10}Be(OH)$_2$ diffuses through the atmosphere until it attaches to an atmospheric aerosol. Precipitation cleanses the atmosphere of ^{10}Be attached to aerosols to a degree that is not currently known (Field et al., 2006; Zhou et al., 2007). When delivered to an aqueous environment, ^{10}Be is ultimately scavenged from non-acidic water on settling particles and deposited in marine and lacustrine bottom sediments where it decays with a half-life of 1.39 million yr (Nishiizumi, 2007; Chmeleff et al., 2009; Korschinek et al., 2009). When ^{10}Be is delivered by snow, rain or by dry

deposition to a site, it adsorbs to soil particles. The high reactivity of hydrolyzed ^{10}Be at most natural pH levels ensures that meteoric ^{10}Be is readily adsorbed to particles (Fig. 1) in the upper meters of soil profiles. Water may liberate ^{10}Be over time although the conditions for dissolution of ^{10}Be are debated. *In situ* production of nuclides in these settings is not a problematic measurement interference because 'meteoric' ^{10}Be is produced in much larger quantities compared to *in situ* production in quartz (meteoric flux = ca. 1 million atoms cm^{-2} yr^{-1}; *in situ* production = ca. 2-20 atoms g $quartz^{-1}$ y^{-1})(McHargue and Damon, 1991; Gosse and Philips, 2001) and because the two varieties of ^{10}Be can also be easily separated through chemical stripping of the outside of the grain (for meteoric) and dissolution of the crystal lattice (for *in situ*). The following sections describe the details of the above processes and intend to quantify the various uncertainties and scenarios that lead to variations in observed ^{10}Be concentrations on the Earth's surface.

2.1.Quantifying the atmospheric flux

2.1.1. Production

The flux of atmospheric ^{10}Be to the Earth's surface varies over time and space as a function of both changes in production of nuclide in the atmosphere and delivery of those nuclides to the surface. Production variations arise from changes in the intensity and orientation of the geomagnetic field, which blocks all but the high-energy charged particles (mostly protons) comprising primary galactic cosmic radiation. The geometry of the Earth's magnetic field produces a predictable latitudinal variation (Fig. 2a)(Lal and Peters, 1967; Masarik and Beer, 2009) with more radiation reaching the poles. The field characteristics define the cut-off rigidity which describes the lowest energy particle that can penetrate into the upper atmosphere for a given location and time. For higher rigidities, there is a lower probability that primary particles will penetrate the upper atmosphere. Low-energy solar cosmic radiation (also mostly protons) contributes negligibly to cosmogenic nuclide production even at the poles (cf. Masarik and Reedy, 1995). At these high latitudes, the Earth's magnetic field lines are sub-perpendicular to the land surface and radiation with lower range of energies can pass through the magnetic field. Once the primary particles penetrate the Earth's magnetic field, they initiate a cascade of secondary particles that ends when the particles have lost so much energy that they can no longer cause atom spallation. Successive reactions result in fewer reactions as the particles lose energy in the process. The production rate at the base of a thick atmosphere is lower than the rate in the upper atmosphere because at low altitudes the secondary cosmic ray particles have lower energies and fewer nuclear reactions take place. However, the flux of nuclides at low elevations is higher than the flux at high elevations because the total nuclide flux is determined by the accumulation of ^{10}Be through the atmosphere mass column. Importantly, 99% of the atmospheric nuclide production takes place at elevations of above 3 km (Fig. 2b). Below this altitude, the energy of secondary cosmic rays is too low to induce further spallation reactions in significant amounts. This altitude insensitivity of the production rate and little atmospheric mixing between sea level and 3 km (Kollár et al., 2000) offers a distinct advantage over *in situ* ^{10}Be applications since meteoric ^{10}Be production rates do not require altitude scaling beneath this altitude. Even near the top of the atmosphere, the number of target particles is not limiting the rate of production. Rather, the intensity of the cosmic ray flux, in particular at low geomagnetic cut off rigidities, exerts the dominant control on the atmospheric production.

Since the original work on meteoric ^{10}Be in the 1980s, much progress has been made (Masarik and Beer, 1999; 2009; Kollár et al., 2000; Reedy, 2000; Webber and Higbie, 2003; Webber et al., 2007) modeling predicted fluxes of ^{10}Be through the use of advanced rigidity models for predicting the radiation received at the top of the atmosphere and through the use of cascade transport codes for predicting the spallation production of nuclides through the atmosphere. Such models use a Monte Carlo approach (Masarik and Reedy, 1996) to model the cosmic ray flux through the atmosphere. These simulations of the production processes (Masarik and Beer, 1999; Masarik and Beer, 2009) predict the amount of cosmogenic radionuclides produced as a function of solar activity, geomagnetic field intensity, altitude and geomagnetic latitude. Masarik and Beer (1999) have produced curves of production rate at various given atmospheric thicknesses for given latitudes. We can transpose these into a latitudinally banded flux for specific altitudes (Fig. 2a). The combination of increased flux toward the poles and the increasing thickness of the atmosphere for low latitudes and the low-pressures at the poles results in a maximum at mid-latitudes. With low altitudes, nuclide production becomes negligible, and the nuclide flux to the surface is mostly that produced on the upper troposphere and stratosphere (Fig. 2b). At the present time, the largest uncertainty in cosmogenic nuclide production rate models is the uncertainties in the nuclear cross-sections and excitation functions for nuclides produced by high-energy neutrons (Kollár et al., 2000). Despite these uncertainties (Kollár et al.,

2000), modeled fluxes with atmospheric transport (see §2.1.2 below) match empirical measurement in many cases. Ongoing measurements of neutron cross sections (Nishiizumi et al., 2009) will likely decrease this uncertainty in future production models.

2.1.2. Delivery

Early on, it was understood that atmospheric circulation that influence the precipitation rate and/or the atmospheric transport to an area could potentially cause the production signal to deviate from that predicted by simple integration of the production rates in a column of air above a site (Lal, 1987; Beer et al., 1988). Current atmospheric mixing models differ in the way they predict ^{10}Be transport (see, e.g., discussion by McCracken, 2004). These mixing models range from limited mixing (only above 60° latitude as in Bard et al., 1997 and Usoskin et al., 2003 and M1 in McCracken, 2004) to complete atmospheric mixing (akin to Carbon-14 mixing models, although without hemispheric mixing as in Beer, 2000 and the M6 model of McCracken, 2004) and various intermediate mixing scenarios. There is also no consensus from the literature what exact effect precipitation has on the ^{10}Be flux to an area. In Central Greenland for example, Yiou et al. (1997) observed roughly doubled ^{10}Be concentrations during periods of halved snow accumulation, implying a *dilution* effect, such that with more precipitation the flux remains constant. More recently, however, Zhou et al. (2007) linked a non-magnetic-field-related portion of the observed change in ^{10}Be flux in loess profiles through time to presumed large precipitation variations. This climate effect in a loess deposit may show an *additive* effect, such that with more precipitation the flux increases and vice versa. L. Brown et al. (1989) found that over the time scales of storm events, there was no positive correlation with Mauna Loa precipitation rates and the meteoric ^{10}Be concentration in that rain. The debate as to whether a given site shows a precipitation *dilution* effect or an *additive* effect is made more difficult by an analysis in which the flux of ^{10}Be into a given site is plotted as a function of the accumulation rate. This analysis introduces spurious self-correlation because flux is the product of concentration and accumulation rate itself (and a density term). Thus far, the unknown effect of the dependence of precipitation on the scavenging of ^{10}Be has made it more difficult to ascribe specific causes to changes in the ^{10}Be ice core and high-resolution sedimentary records without independent knowledge of geomagnetic field strength (Wagner et al., 2000) or solar cycles (Wagner et al., 2001) from radiocarbon in the same deposits (Muscheler et al., 2000) and other methods. From these studies and others, it is now possible to distinguish changes in nuclide production, such as fluctuations in solar modulation of primary cosmic rays and geomagnetic field intensity, from climate-related changes in nuclide delivery (Field et al., 2006).

To evaluate these competing influences of ^{10}Be production and delivery quantitatively, we rely on the recent work of Field et al. (2006) who used the Goddard Institute for Space Studies ModelE (GISS) general circulation model (GCM) and Heikkilä (2007) who used the European Centre for Medium-Range Weather Forecasts-Hamburg Model 5 (ECHAM5) GCM in combination with Masarik and Beer's (1999) production functions. These authors evaluated the effect of specific climate controls over the ^{10}Be concentration signals in ice cores. Such models are necessary because processes that affect the distribution of ^{10}Be in the troposphere, such as changes in stratosphere-troposphere exchange or aerosol scavenging efficiency may change with changing climate over the globe. Figure 3 shows a mean of Heikkilä (2007) and Field et al. (2006) flux results, but adapted for the long-term solar modulation factor (700 MeV) and long-term average geomagnetic field strength (M=0.75). Long-term geomagnetic field values for Heikkilä (2007) were recalculated from those published to show the long-term geomagnetic field by latitude. We used Figure 5 of Field et al. (2006) for this conversion. Field (pers. comm.) provided annual mean wet and dry ^{10}Be deposition averaged over 30 years, with "average" cosmogenic production conditions (phi = 700 MeV) and a pre-industrial atmosphere and so no adjustment was necessary for her calculated fluxes.

The latitudinally averaged flux for Heikkilä (2007) and Field et al. (2006) and the percentage difference ^{10}Be flux between the two agree relatively well with zones of storm tracks showing highest flux due to effective mixing of ^{10}Be-rich air from the stratosphere into the troposphere. The zone which shows the greatest difference is the equatorial region which the Heikkilä (2007) model shows to be a region of ~20-50% higher ^{10}Be flux due to increased storm activity in the ECHAM5 GCM relative to the GISS GCM used by Field et al. (2006). In contrast, Field et al. (2006) estimate a generally ~30% higher flux in the Northern Hemisphere. However, the mean flux over the Earth, 5.8×10^5 ^{10}Be atom g^{-1} cm^{-1} y^{-1}, is similar for both models and is identical to that predicted by Masarik and Beer (1999). This globally averaged flux was prescribed for both models.

Fortunately, we can measure ^{10}Be concentration in certain records where the accumulation rates or rates of rain or snowfall are known (Fig. 4). Substantial variability normally observed in the ^{10}Be concentration from precipitation measurements reflects short term fluctuations in precipitation rate, stratosphere/troposphere exchange, magnetic field strength, varying ratios of dry versus wet Be deposition, and incorporation of recycled ^{10}Be (dust) into precipitation collectors (Yr et al., 1985/86; Graham et al., 2003). At first sight, this scatter appears to prevent assignment of a consistent flux to a given location. However, ^{10}Be concentration in rain measured over 2 yr for New Zealand sites (Graham et al., 2003) and over 4 yr for Switzerland sites (Heikkilä et al., 2008) show a distinct relationship between the amount of precipitation, and the concentration of meteoric ^{10}Be (Fig. 4a, b). The black line is the best fit line and the value of the slope of the correlation between the concentration and the inverse of the precipitation rate is equal to the value of the flux of ^{10}Be. The y-intercept provides the initial ^{10}Be loading of precipitation by a recycled ^{10}Be source such as, for example, ^{10}Be adsorbed to small amounts of entrained dust. In the case of the rain experiments, the flux roughly matches that predicted by Field et al. (2006) and Heikkilä (2007)(Table 1). In the case of the Japan terrace site (Maejiima et al., 2006), there is a factor of 2 difference between the predicted flux and the measured flux. In this case, the coupling of the coarse model resolution and small scale climate perturbations from may prevent a better flux estimate in this area.

The inferred flux values appear to be independent of altitude, as predicted by negligible production at altitudes < 3 km (Fig. 2b). For example, precipitation data from Switzerland (Heikkilä et al, 2008) yields identical fluxes at Jungfraujoch at 3580m as in the Swiss Mittelland at 440m (Fig. 4b, Table 1). In paleo-^{10}Be records, such as in ice cores (Fig. 4c), both the concentration of ^{10}Be and the accumulation rate of the material must be independently known. A long-term record of ^{10}Be precipitation is provided by concentration measurements of ^{10}Be and in the GISP2 and GRIP ice cores, respectively, versus the inverse of the ice accumulation rate (Fig. 4c). The derived flux also matches the Field et al. (2006) and Heikkilä (2007) modeled prediction and shows a dilution of the ^{10}Be flux by variable volumes of water. Although these records at coastal, island and high elevation continental interiors (Fig. 4a and 4b) show dilution of the ^{10}Be flux, in other settings precipitation may scavenge the atmospheric ^{10}Be differently. Most early studies (e.g., Yr et al., 1985/86; L. Brown et al., 1988) concluded that for mid-latitude sites with moderate precipitation rates, the ^{10}Be concentration in precipitation is approximately constant, and the flux should be calculated as the average global flux (atom cm^{-2} y^{-1}) per 100 cm annual rainfall. However, in regions of high rainfall (greater than 6 to 10 cm month^{-1}) ^{10}Be may be fully extracted from the atmosphere. Unfortunately, global records of ^{10}Be concentrations coupled with data on the delivering agents and their environments are not available (and would be quite costly!) to test this precipitation scaling.

Instead, we can consider settings in which the effect of production changes in certain records of Beryllium-7 (^{7}Be) concentrations where the rates of rain or snow deposition are known (Fig. 5). These records are convenient because ^{7}Be acts chemically similar to ^{10}Be in terms of the droplet scavenging processes and mixing processes between the upper and lower atmosphere. In some settings where atmospheric transport times are short, the ^{10}Be and ^{7}Be concentration in rain can be well-correlated ($r > 0.7$: 'Knies et al., 1994). However, the use of ^{7}Be records for understanding ^{10}Be delivery is not exactly correlative because ^{7}Be decays with a half-life of only 53 days, which is the same order of magnitude over which some atmospheric cycling processes occur. Thus, in some environments with complex atmospheric cycling, the changing concentrations of ^{7}Be reflect both scavenging processes and residence time in the atmosphere (Raisbeck et al., 1981a,b). With this in mind, Feely et al. (1986) published a large dataset of ^{7}Be concentrations for a variety of settings such as hinterlands, islands, and coastal areas for a range of altitudes and latitudes. Such settings have a range of dominant atmospheric transport times and so we can attempt to separate the effects of transport time, transpiration and precipitation.

Monthly rainfall and fallout concentration trends for island settings and most coastal settings are best described by a *dilution* of ^{7}Be fluxes (and presumably ^{10}Be fluxes) by variable rates of precipitation. The correlation of the inverse of rain rate and ^{7}Be concentration collected at island stations or coastal locations may indicate that, regardless of the rain rate, precipitation directly from the ocean strips most of the available ^{7}Be from the atmosphere (Fig. 5a, 5b) unless the site receives ~ less than 6-10 cm month^{-1} of rainfall for mid-latitudes and 0.5-1 cm month^{-1} for high latitudes. This scheme is consistent with clouds forming quickly and raining-out completely (Fig. 6a, b). In this case, increasing the amount of moisture received does not necessarily increase the amount of ^{7}Be to the site. Some high elevation

sites within continental settings (Fig. 5c) seem to demonstrate this *dilution effect* as well. We observe this trend for the GISP2 ^{10}Be record (Fig 4c). In some cases, the concentration of ^{7}Be is constant regardless of the amount of rain (Fig 5d). This case may be explained by ^{7}Be-poor water vapor returned to the atmosphere by transpiration. Low-elevation sites within continental settings (Fig. 5d) typically show an *additive effect*. In these settings, clouds may contain a certain quantity of ^{7}Be atoms for a volume of water vapor and the flux would increase with precipitation rate (Fig. 6c). Clouds may continually be replenished with ^{7}Be as they travel.

The explanations offered above assume that a large portion of the fallout is delivered through rain. A numerical model which incorporates climate into the predicted global fluxes predicts that the ratio of dry fallout versus wet deposition can range from less than 0.1 to approximately 2 (Field et al., 2006). Measurements of dry fallout to wet deposition of ^{7}Be are typically in the range of less than 10% (Kaste et al., 2002; Wallbrink and Murray, 1994). In a particularly exhaustive study of atmospheric fallout of ^{7}Be measured in dozens of rainfall events at Black Mountain, Australia, Wallbrink and Murray (1994) reported that the activity of dry fallout was found to contribute a maximum of 10% of the wet fallout in any one month. For this same site, Field et al. (2006) model a ratio of dry to wet deposition 0.5 for ^{10}Be. Of course in extreme cases, where no precipitation falls such as the South Pole Station, Antarctica, Feely (1989) noted that the ^{7}Be still was deposited as either very concentrated ^{7}Be frost or completely in the form of dry fallout.

Presumably, in coastal and island settings where the atmospheric transport time is fast and ^{10}Be and ^{7}Be concentrations in rain are significantly correlated with precipitation rate, the yearly flux of meteoric ^{10}Be is independent of the rain rate (Fig. 6c). In these cases of constant flux, predictions of ^{10}Be flux over time are not limited to our knowledge of past precipitation rates, which is quite encouraging for applications of ^{10}Be techniques in modern and past sedimentary deposits where precipitation rates are likely to have changed.

The analysis presented above is even more encouraging inasmuch as most of the recent ^{10}Be flux estimates (Table 1) agree with those predicted from the combined production delivery models (Fig. 3). How then, do we treat the secular variations introduced into the production of cosmogenic nuclides by variations in the solar modulation function Φ and geomagnetic field strength? ^{10}Be measured in ice cores and ocean and lake cores have been used for reconstructing these parameters (Steig et al., 1996, Frank et al., 1997; McCracken et al., 2004; Vonmoos et al., 2006; Muscheler et al., 2007; Ljung et al., 2007). We see that as a result of these solar and field strength variations, ^{10}Be concentration in continuous ice (Vonmoos et al., 2006; Muscheler et al., 2005) and sediment layers (Frank et al., 1997) can deviate up to 40% (from minimum to maximum). The integrated effect of temporal changes resulting from solar modulation is thought to be minimal, however, when measured over the presumably long (ky) time periods over which ^{10}Be accumulates in soils. This case is best illustrated by the variations in ^{10}Be flux as recorded over the past 10 ky in the GRIP ice core (Vonmoos et al., 2006)(Fig. 7). While the measured flux at any single point in time can vary by some 30% to that ca. 100 yr before or after this measurement, the long-term integrated flux is not affected by these short-term fluctuations and is identical to that predicted by the solar modulation-normalized models (Fig. 3). Given that soils accumulate ^{10}Be over similar integration time scales, solar modulation is not of concern for soil and sediment tracing studies. Variations of the geomagnetic field strength, in contrast, operate over much longer time scales. We can use measured ocean records (Frank et al., 1997) and production/delivery models (Field et al., 2006; Heikkilä, 2007; Masarik and Beer, 2009) to correct for these effects, as is done in measurements of cosmogenic nuclides produced *in situ* (Gosse and Philips 2001).

2.2. Dust

Wind can remobilize ^{10}Be from its resting place in the form of dust. Dust introduces another component to the flux of ^{10}Be into the soil and out of the soil. In natural systems, the meteoric flux (wet and dry deposition) and the aeolian flux comprise the total deposition of ^{10}Be. Therefore,

$$Q_{total} = Q_{meteoric} + Q_{dust} . \quad [1]$$

In the case where we have independent information to constrain both the time-integrated flux of ^{10}Be and dust content such as in ice cores and rain experiments, we find that the average estimated flux of

^{10}Be from dust to be on average ~1.5x10^{6} atoms g(rain)$^{-1}$ (Graham et al., 2003) in New Zealand rain traps and ~1x10^{4} atoms g(ice)$^{-1}$ in Greenland ice cores (Lal, 2007). These values correlate well with the y-intercepts in Figure 4. Using the technique of Lal (2007) in ice cores from Antarctica and Greenland, the dust flux can be estimated indirectly by correlation with the Calcium concentration. Using this technique, dust contributes a flux of <5% of the total ^{10}Be flux to Greenland ice during the Holocene and <20% of the total ^{10}Be flux during the highest dust flux times. In Antarctic cores, the dust contributes only <1-6 % of the total fallout. In a plot of inverse accumulation rate vs. ^{10}Be concentration (e.g. in Fig 4c), the value of the y-intercept may give the average dust ^{10}Be concentration in the ice. This value is similar to the dust concentration measured reported in Yiou et al. (2002).

Away from high ice domes, the dust flux is not well characterized and can range from extreme settings (e.g. loess belts) to low dust input settings (mountain peaks). The upper bounds for the measured concentration of ^{10}Be in dust is 10^{10} atoms g^{-1} (Baumgartner et al., 1997). In the equatorial Pacific, glacial dust fluxes are about a factor of 2.5 higher than interglacial fluxes (Winckler et al., 2008). At the poles, glacial to interglacial fluxes have a variability of over a factor of 20-50 times higher (EPICA, 2004; Sugden et al., 2009) than the equatorial samples. However, the concentration of ^{10}Be in dust ultimately depends on the soil residence time of the dust source area and the grain-size of dust. For example, dust sourced in areas of active glaciation potentially carries much lower ^{10}Be loads (10^{4} atoms ^{10}Be g^{-1}), due to shorter residence times (Shen et al., 1992, Balco, 2004, Sugden et al., 2009). Conversely, relatively highly ^{10}Be-loaded dust (10^{8} atoms ^{10}Be g^{-1}) can originate from exposed continental shelves due to lowered sea levels. During the Holocene in most locales outside of loess belts, the annual dust flux is found to be approximately 10^{-4} g cm^{-2} y^{-1} (Prospero, 1999; Jickells et al., 2005). Considering the rare, upper bound concentration of 10^{10} atoms g^{-1}, the resulting dust depositional flux would be approximately equal to the atmospheric fallout flux derived from precipitation. However, concentrations of ^{10}Be in dust of 10^{10} atoms g^{-1} (Baumgartner et al., 1997) are extreme and also a function of grain-size such that only the finest material would be so loaded with ^{10}Be. Lower measured concentrations of ^{10}Be in dust (Gu et al, 1996; Graham et al., 2003) are similar to those in soils (10^{4} - 10^{8} atoms g^{-1}: Lal, 1999) – such that outside of loess belts or during the Holocene – these fluxes of ^{10}Be from dust are orders of magnitude lower than the atmospheric fallout and are not considered a source of great uncertainty.

2.3.Retentivity

Once meteoric cosmogenic ^{10}Be atoms from the atmosphere reach the ground they bind very tightly to soil and sediment particles due to the reactive nature of $Be(OH)_2$. However, unlike *in situ*-produced ^{10}Be, which is always hosted and locked to 100% in quartz, meteoric ^{10}Be is retained only under certain chemical and mineralogical boundary conditions. Although under most conditions this is the case, exceptions exist in which ^{10}Be is lost into the dissolved phase. It is important to identify such settings. A wide range of approaches has been used to characterize the retention behavior of Be in soils. These are speciation of dissolved Be, the nature and chemistry of the sites of adsorption, the exploration of depth-distribution of Be percolation into soils, an analysis of the grain size dependence of ^{10}Be adsorption, and a comparison of the predicted ^{10}Be inventory with that found in soil chronosequences. For the transport of ^{10}Be adsorbed to river suspended loads, it is critical to evaluate whether all nuclides eroded from hillslopes are indeed carried by river particles, or whether they might be desorbed, thereby entering the dissolved phase. The approaches used to determine these last two issues are partition coefficients and the establishing of watershed mass balances and are reviewed here.

2.3.1. Speciation

Figure 8 shows that in the absence of humic acid, above a pH of 5, most Be is present as the hydrolyzed species. Given the reactive nature of this hydroxide, any dissolved ^{10}Be is likely to be adsorbed readily onto clay minerals and iron oxy-hydroxides. In the presence of humic acid, as is the case in many organic matter-rich soils, Be is present as a humate complex from a pH of 3 to 11 (Takahashi et al., 1999). Like many other negatively charged metallo-organic complexes, Be humate complexes are very reactive because they have a high affinity to be adsorbed onto positively charged Fe-oxy-hydroxides, Al hydroxides, and clay minerals. Consequently, Takahashi et al. (1999) have observed that 70% of dissolved Be is adsorbed as humate complex to kaolinite at pH 7.5. Gustafsson et al. (2003) have further suggested that natural organic matter (NOM) itself is an important sorbing agent for metals in many surface horizons in soils, and have shown that Zn, Cd, Ca, Pb, Cu, and Mg are adsorbed at a pH > 4.

To summarize, $Be(OH)_2$, and organic-Be complexes are both likely to be immobile at pH > 4.

2.3.2. Adsorption characteristics in soil

At a pH < 4.1, soil solutions are under-saturated with respect to gibbsite $Al(OH)_3$, such that Al^{3+} will be soluble (Berggren and Mulder 1995). The released Al^{3+} competes with other metals for exchange sites, potentially resulting in release of these competing metals, amongst them Beryllium, into solution. In the Beryllium literature, it is frequently mentioned that soils are "saturated" with respect to Beryllium. We regard it as unlikely that the low concentrations of ^{9}Be (1-3 ppm in crustal rocks and soils), plus the few atoms of ^{10}Be, can lead to saturation of adsorption sites. Rather, we suggest that at pH < 4 it is the competition with dissolved Al for exchange sites that might result in partial release of Be.

The presence of colloids can also cause Beryllium mobility. Because of their large surface area, mobile colloids can serve as excellent transporters of adsorbed metals in aqueous fluids. With regards to colloid stability, the presence of natural organic matter (NOM) increases mobility of Beryllium because NOM increases colloidal stability hence decreases the filtering capability of saprolite to retain metals (Kretzschmar et al., 1995). Similarly, redox cycles increase colloid stability by increasing pH-induced colloid dispersion (Thompson et al., 2006) and may help keep ^{10}Be mobile.

In summary, below a pH of 4, Al can compete with Be for exchange sites. Well-oxidized soils that are not subject to frequent redox cycling serve to retain Be as they prevent colloid stabilization by redox cycles. The primary determinant of whether Be is retained in soils is the hydrology of soils. Only in soils that are exposed to sufficient water will dissolved Beryllium be lost into groundwater and potentially into river water. Be is likely to be retained at the surface of soils.

2.3.3. ^{10}Be in plant litter and sediment rich in organic carbon

As yet, no consistent observational data set exists that describes the way in which ^{10}Be transport or retention is affected by biogenic organic carbon, and in particular by plant litter. One report of ^{10}Be concentrations of 10^{10} atom g^{-1} in hand-picked organic matter from river and lake sediment by Lundberg et al. (1983) would indicate that organic materials accumulate large amounts of ^{10}Be, as this concentration is many orders of magnitude higher than soils exposed for a similar amount of time. Lundberg et al. (1983) also found that >90% of the ^{10}Be was contained in the organic, H_2O_2-leachable phase in lake sediments. In contrast, in one measurement of ^{10}Be in living plant material, ^{10}Be concentration of hardwood is only 10^6 atom ^{10}Be g^{-1} (L. Brown, 1984), which does not imply enriched amounts of ^{10}Be within that living material. We can compare these observations with measurements of the stable isotope ^{9}Be in the cycle of organic matter. Although measurable in many cases, the overall uptake of Be is low (Meehan and Smythe, 1967) - even in acidic soils where it is more mobile (Keilen et al., 1977). Keilen et al. (1977) reports that Be does not take part in the organic matter metal cycle as do other metals like Pb and is not enriched in the soil humus.
In summary, we still do not understand the magnitude or the timing of the concentrating effect of ^{10}Be in organic matter in soils which is a topic worthy of future study.

2.3.4. ^{10}Be distribution with depth

The migration of solutes through a soil profile (e.g. Freeze and Cherry, 1979) is often described as a chromatographic column where the nuclide of interest is continuously added at the top of the column and eluted. E. Brown et al. (1992) suggested this model for the diffusion of ^{10}Be into a soil. Redistribution of the nuclide through the column is retarded by both high distribution coefficients and low soil porosity. For young (i.e. recently-exposed, glacial) sediments, the downward migration can be described well with an exponential adsorption law. The equation for the exponential function can be written:

$$N(z) = N_{surf} e^{-zk} \qquad [2]$$

where N(z)[atom g^{-1}] is the ^{10}Be concentration at depth z [cm], N_{surf} is the surface concentration, and k an adsorption coefficient [cm^{-1}] describing the decrease of nuclides with depth, and 1/k is the relaxation

depth scale [cm]. k describes the shape of the ^{10}Be depth distribution for a soil profile with a homogenous grain-size distribution and constant subsurface density. The length scale of the 'attenuation' of the concentration with depth is just the e-folding depth for the exponential decrease of the ^{10}Be with mass depth (Blake et al., 2002) and is based solely on empirical data (See Fig. 9a: Balco, 2004). The meaning of such a exponential relationship may be related to: (a) simple downward solution advection and diffusion of ^{10}Be-bearing water from precipitation, (b) organic-material concentrations in the soil, (c) the presence of wetted pathways during downward percolation of water (Deurer et al., 2003), (d) random walk-type adsorption onto soils with fractal grain-size distributions (Gregg and Sing, 1982), and (e) remobilization of ^{10}Be due to the dissolution of chemically weathered minerals and unlocking of their associated ^{10}Be sites. These possibilities are neither exhaustive, nor well-known and they are difficult to test either in the field or under laboratory conditions that mimic natural soil profiles. Clearly, this is an area for further research. Regardless of the physical process responsible, the empirically derived relationship may still be used for quantifying soil transport processes. In measured soil profiles, the depth-scale (1/k) constants range from 5 mm to 50 cm and depend mostly on the grain-size of the substrate (Fig. 9).

2.3.5. Grain-size

In most soils with homogenous grain-size distributions with depth, ^{10}Be concentrations have a surface maximum that decreases monotonically with depth (Pavich et al., 1984, 1986) (Fig. 9a,b). Soils with a subsurface B_t (eluviated clay-rich) horizon have a mid-depth maximum ^{10}Be concentration (Fig. 9c). This mid-depth maximum is typically a result of smaller grain sizes. The smaller grain sizes often have a greater surface area per unit mass and enhanced ion exchange capabilities (E. Brown et al., 1992). Concentrations may be normalized for this increase in grain size per unit of mass. The normalization can be described with the following power-law function (Eq. 3) imported from short-lived fallout ^{210}Pb, ^{137}Cs and ^{7}Be nuclide techniques (He and Walling, 1996; Wallbrink and Murray, 1996):

$$N_{adjusted} = N_{measured}\left[\frac{S_{measured}}{S_{reference}}\right]^{\gamma} \qquad [3]$$

where $N_{adjusted,\ measured}$ are the ^{10}Be concentrations for the adjusted and measured samples and $S_{reference,\ measured}$ are the surface areas of a reference and measured sample and the γ is a factor that describes the non-linear particle-size selectivity of the sorption process. The power law exponent that describes the relationship between grain-size and ^{10}Be concentration for grains larger than 3 μm is approximately -0.5 +/- 0.1 in many environments (Fig 10). Grains below this size obtain a uniform concentration of ^{10}Be. The γ value is thought to be loosely lithology-specific as it is for shorter-lived fallout nuclides (He and Walling, 1996). Similar grain-size dependencies of the ^{10}Be, ^{7}Be and ^{210}Pb concentrations are well documented (Shen et al., 1992; Gu et al., 1996; He and Walling, 1996; Blake et al., 2002; Shen et al., 2004, Maejima et al., 2005). Much past pioneering work using meteoric ^{10}Be as an erosion rate proxy (Valette-Silver et al., 1986; L. Brown et al., 1989) neglects this effect of grain size, does not correct for the variability in grain-size change during erosion events, or does not fully measure the smallest particles of the clay fraction (5-64 μm) where the ^{10}Be concentration can vary greatly.

In their study of provenance of fine-grained sediments,: Helz and Valette-Silver (1992) and van Geen et al. (1999) made provisions for this grain size effect to determine potential differences in source area by normalizing the measured ^{10}Be concentrations to Fe (iron) concentrations. In these studies, the greater the ^{10}Be concentrations were associated with greater iron concentrations. These correlations between ^{10}Be and Fe concentrations are likely to be controlled by oxy-hydroxides providing Beryllium exchange sites.

The concept behind using a metal concentration to normalize for differences in ^{10}Be scavenging and particle-specific adsorption characteristics was insightful. Iron, however, is a questionable candidate for a perfect normalizing metal because of iron's two different redox states. When choosing a normalizing metal, some metals are better suited than others. An ideal candidate for normalizing meteoric ^{10}Be would have as many as possible of the following characteristics: 1.) the metal should behave chemically similar to ^{10}Be such that the distribution coefficient (K_d) is close to or exactly the same as that of ^{10}Be; 2.) the metal should not provide additional sites for ^{10}Be adsorption; 3.) the supply of the metal should not be limiting its flux onto adsorption sites; 4.) the metal should not be available in

overloading quantities such that exchange sites become saturated. A particularly well-suited normalizing element would be Beryllium itself (stable ^{9}Be). Normalizing meteoric ^{10}Be has become almost common practice in ocean studies by using ratios of authigenic (adsorbed) ^{10}Be/^{9}Be to adjust for differences in particle reactivity and changes in scavenging and particle availability with time (Bourlès et al., 1989; Barg et al., 1997; Frank et al., 1997). However, a prerequisite to using adsorbed stable ^{9}Be is the selective extraction of the adsorbed species and its separation from that bound in 1-3ppm concentrations within the lattice of silicate minerals (Bourlès et al., 1989).

When measuring ^{10}Be in river sediment as an erosion rate proxy (see below for details), a clay sample will have an order of magnitude higher concentration of ^{10}Be as compared to a sand sample from the same catchment because of the great differences in surface area for the same weight of sample (Fig. 10). In this case, either a normalizing metal must be used to adjust for this effect or at least two samples with differing grain size must be analyzed to measure the non-linear affinity of ^{10}Be for smaller grains. Understanding this change in grain size is crucial for quantifying changing erosion rates through time instead of merely changing grain-size as a function of time. However, the grain size effect does not affect methods that measure the entire ^{10}Be inventory.

2.3.6. Chronosequences

Retentivity of ^{10}Be in soils is best assessed if the age of a soil is known from independent estimates, and its meteoric ^{10}Be inventory is measured. If the production rate is known, then the inventory can be predicted. If the measured inventory agrees with the predicted one, then all ^{10}Be was retained. This situation seems true for some of the chronosequences listed in Table 2. If, on the other hand, the inventory suggests a deficit of ^{10}Be, then it was suggested that "saturation" with respect to ^{10}Be has been reached (E. Brown et al., 1992). This "saturation" is usually observed when the soil profiles are extremely old ($>10^{6}$ yr), which is probably due to the occupation of adsorption sites by competing elements (see §2.3.2). In these cases, the concentration of meteoric ^{10}Be can be constant with depth. However, alternative explanations are possible for the observed deficit: (1) in some cases, observed saturation may be a result of assigning zero erosion rates to surfaces which are steadily – albeit slowly – eroding as seen in Table 2; (2) the age estimate can be in error which would result in a wrong accumulated inventory; (3) if the age estimate is in error and the soil is also old ($>10^{6}$ yr) then the time-integrated radioactive decay of ^{10}Be can be in error; and (4) there may have been lateral redistribution of ^{10}Be along water-sealing soil layers, or trapping of ^{10}Be imported laterally by layers rich in particle-reactive mineral surface. Yr et al. (1983) inferred from a lack of ^{10}Be in dated terrace material that the residence time of ^{10}Be in soils was only 5-40 x 10^{3} yr. However, in such old terraces (>100 x 10^{3} yr), an erosional loss could easily explain such a lack of ^{10}Be. This possibility will be discussed in more details in §3.2.

2.3.7. Partition coefficients

Beryllium is particularly reactive in natural soils. The reactivity of Be can be quantified by measuring the ratio of concentrations of a compound adsorbed to solids to the concentration of the tracer in solution in equilibrium and is referred to as the partition coefficient, K_d. Hawley et al. (1986) reviewed partition coefficients (K_d) of Beryllium in the marine system to be around 10^{4}. Partition coefficients between fresh water from Lake Michigan and suspended sediment were much higher, ranging from 10^{5} to 10^{7}, inversely related to the concentration of total solids in solution. You et al. (1989) have also investigated the pH dependence of partition coefficients and found that K_d is 10^{5} at pH > 6, 10^{4} at pH 4 to 6, and 10^{2} to 10^{1} at pH < 4. These observations were made for ^{7}Be adsorption from river water onto kaolinite, illite, and natural river mud. Similar observations were made for sorption of Be into biotite and albite (Aldahan et al. 1999). At a pH of 6, K_d on biotite is 10^{3}, while that of biotite was 10^{2}, and increased to > 10^{5} for both minerals at a pH of 9. Importantly, in a dissolution experiment, Be sorption increased with increasing biotite dissolution indicating generation of further adsorption sites during mineral weathering. You et al. (1989) also investigated the increase of K_d with time, and the highest K_d is usually reached within only 7 days for both river suspended sediment and soils. The interval of 7 days appears, at first sight, a long period to allow for redistribution of Be. However, this period allows for Be to travel to these sites in soils where retention will eventually be ensured. This could be at sites of high pH or small grain-sizes. These measurements based on ^{7}Be confirm the predictions made above: at pH > 4, ^{10}Be adsorption onto clays is strong, and also fast.

2.3.8. Watershed mass balances

Heterogeneities in retention are averaged out on the watershed scale. One important empirical way to assess retention of Beryllium in soils is to balance the flux of dissolved ^{9}Be and ^{10}Be exported by rivers with that fluxed into a watershed by weathering (^{9}Be) or precipitation (^{10}Be). The only systematic study done to date is that by E. Brown et al. (1992) who studied tropical rivers of the Orinoco and Amazon basin. In support of the predictions made above, these authors observed high stable ^{9}Be concentrations of 2000 to 6000 pM in rivers with pH of 4 to 6 indicating that Be stays in solution more readily with lower pH values. Concentrations decreased to < 500 pM at pH >7. However, some of these elevated concentrations are likely to be caused by ^{9}Be released from silicates during weathering. ^{10}Be provides a much better tracer of retention. First, E. Brown et al. (1992) compared the concentration of ^{10}Be in a local soil profile (~3.5×10^{7} atoms/g soil) with that in local precipitation (~2×10^{3} atoms/g) to derive a partition coefficient of 1.5×10^{4} for a pH of 4.5. This value agrees well with the experiments by You et al. (1989). Second, dissolved ^{10}Be concentrations of 13 rivers were provided. Of these, the low-pH (4-6) rivers Cuchivero, Orinoco, and Negro contained high dissolved ^{10}Be concentrations of 1000 to 3200 atoms/g. When corrected for evaporation, these concentrations are similar to those of the regional precipitation, suggesting that ^{10}Be is not being retained in soils. ^{10}Be concentrations in the neutral to alkaline Apure catchment waters were low, suggesting that meteoric ^{10}Be is being retained in these catchments' soils.

^{10}Be and ^{9}Be concentrations were measured in Arctic river water. Frank et al. (2009) found that the Mackenzie, Lena, Yenisey and the Ob rivers export approximately one-tenth to half of the annual atmospheric ^{10}Be flux into the drainage basin in dissolved form out of the basin. Some of this dissolved exported meteoric ^{10}Be may even be derived from chemical dissolution of particles eroded from the basins. In the Lena, Yenisey and Ob, the dissolved loads make up ~70% of the total denudation rate determined from combined river particulate and dissolved load fluxes (Summerfield and Hulton, 1994). These catchments could also have return fluxes of meteoric ^{10}Be that are higher than most rivers because large portions of the catchments are composed of permafrost preventing infiltration and because water derived from snow melt may not interact much with the underlying soil column.

The flux of ^{7}Be in river and lake water was also used and compared to that in river particles and the inventory in lake sediments. Kaste et al. (2002) reviewed these and found that in most environments, 95% of ^{7}Be introduced from the atmosphere is found adsorbed to particulates. This lends strong support to the suggestion that in most environments ^{10}Be is also retained and that the three rivers found by E. Brown et al. (1992) and some Arctic Rivers where this is not the case might be exceptional.

3.1. Soil ages from an inventory of ^{10}Be

Once the flux of meteoric ^{10}Be is known or can be estimated within certain limits, and the total amount of ^{10}Be can be measured, the soil age can be calculated. The soils age is the time since its initial exposure (by, e.g., deposition of fresh glacial till, tectonic faulting, or a lava flow) to precipitation. The inventory of meteoric ^{10}Be, I [atoms cm^{-2}], can be calculated by equation 4, where z is the depth to the bottom of the soil column, $N(z)$ is the concentration of ^{10}Be atoms at depth [atom g^{-1}], z [cm], and ρ the soil density [g cm^{-3}].

$$I = \int_0^z N(z)\rho \, dz \qquad [4]$$

If we assume that the atmospheric flux of ^{10}Be, Q(t) [atoms cm^{-2} y^{-1}] at a given site is known, and fluctuates with time by, for example, magnetic field variations, then the soil's inventory relates to the soil age, t, the erosion rate (and hence the rate at which ^{10}Be is lost from the surface), and radioactive decay by the following equation.

$$\frac{d}{dt} I(t) = -\lambda I(t) - N_{surf}(t)\rho E(t) + Q(t). \qquad [5]$$

$$\text{decay} \qquad \text{erosion} \qquad \text{flux}$$

where λ is the radioactive decay constant of ^{10}Be, and E(t) is the erosion rate of the surface (cm y^{-1}) that can vary with time, and N_{surf} is the ^{10}Be concentration at the surface of the soil (atoms g^{-1}). Let's also assume that Q(t) fluctuates around a nearby mean value such that Q(t)= Q, and the surface is not eroding such that E(t) =0, then integration of [5] yields:

$$I = \frac{Q}{\lambda}\left[1 - e^{-\lambda t}\right]. \qquad [6]$$

This equation allows the calculation of the age of very stable, non-eroding soils.

3.2. Erosion rates from an inventory of ^{10}Be

In an eroding or freshly exposed setting, the inventory of ^{10}Be depends on both the initial exposure age of the soil and the rate of soil erosion (because ^{10}Be is continuously removed by erosion). If we assume that the erosion rate is approximately steady such that E(t) = E, the inventory can be calculated from integration of [5] as follows:

$$I = \frac{(Q - E\rho N_{surf})(1 - e^{-\lambda t})}{\lambda} \qquad [7]$$

The age of the soil for various plausible erosion rates can be calculated with the following equation:

$$t = \frac{-\ln\left[1 - \left(\frac{I\lambda}{Q - E\rho N_{surf}}\right)\right]}{\lambda} \qquad [8]$$

Equation 8 contains two unknowns: the age of the soil and its erosion rate. A unique initial exposure age cannot be determined if soils are continuously being eroded for a long period. Similarly, a unique erosion rate cannot be determined if the exposure age is unknown. As in the *in situ* approach (Lal, 1991), we can then eliminate the initial time, *t*, by assuming that a near-infinite time has passed since initial exposure and the system is at steady state between the meteoric flux of ^{10}Be and its removal due to only erosion or radioactive decay. In other words, we assume a steadily eroding setting (for example in an uplifting and eroding mountain belt). The steady state inventory is an inverse relationship between the ^{10}Be content in soil and the local erosion rate defined as (L. Brown et al., 1988):

$$I = \frac{(Q - E\rho N_{surf})}{\lambda} \qquad [9]$$

In young landscape settings that erode slowly, such as in recently deglaciated Minnesota (Fig. 9b), soil has been exposed to ^{10}Be fallout for the last ~15 ky (from glacial retreat ages) and has lost insignificant ^{10}Be atoms from erosion of the surface. This soil contains an inventory of 1.9x10^{10} atom cm^{-2} (Balco, 2004). Assuming a flux of 1.3x10^{6} atoms cm^{-2} y^{-1} for the location from Figure 3a, this results in an age of the soil of ~15 ky that matches well with the regional deglaciation pattern. For these young (i.e. recently-exposed, glacial) sediments, the downward migration can be quite simple such that the surface area scale or the 'attenuation' of the concentration with depth is just the constant for the exponential decrease of the ^{10}Be with depth (See Fig. 9b). Most eroding soils have a high enough clay/silt fraction to retain all the ^{10}Be from precipitation over a local spatial range. The inventory method is insensitive to the depth distribution of ^{10}Be.

3.3. Erosion rates from surface soil concentrations and spatially-averaged erosion rates from meteoric ^{10}Be adsorbed to river sediment

A second application for meteoric ^{10}Be absorbed to sediment could follow the same approach used in applications of ^{10}Be that is produced *in situ* where the production of cosmogenic nuclides in a basin

eventually equals the export of nuclides from a basin through erosion of sediment (i.e. first tested in Granger et al., 1996). In this case, we are not able to measure inventories of ^{10}Be throughout the basin and only want to solve an equation for the erosion rate given a flux and a measured concentration of ^{10}Be at the surface of the soil. We attempt an analytic solution to the differential equation that describes the flux of meteoric ^{10}Be into the system. This solution includes: the downward movement of ^{10}Be into the soil, reworking of ^{10}Be from depth as the top layer is removed by erosion and radioactive decay of ^{10}Be. Assumptions we use to simplify this difficult problem are:

1.) the concentration of ^{10}Be at the surface can be measured,
2.) the retention of ^{10}Be is high, meaning that the nuclide is only lost as adsorbed on particles, and not through solution,
3.) the flux of ^{10}Be into the system is known and is steady on long time scales,
4.) the concentration of ^{10}Be at soil-bedrock interface is practically 0,
5.) ^{10}Be decreases exponentially with depth so that the downward ^{10}Be percolation is dependant on the concentration at each depth interval throughout the soil profile (equation 2).

Note that assumption 2) that of high retention, was explored in § 2.3, assumption 3), that of a steady known atmospheric flux, was justified in § 2.1.2, while assumption 5), that of an exponential decrease of concentration with depth, was justified in § 2.3.4. Later in the derivation, we will also assume that:

6.) the system is at steady state, meaning that the ^{10}Be lost through erosion and decay from the system per unit time is equal to that entering by atmospheric flux,
7.) the erosion rate of the surface is equal to the production of soil from underlying bedrock,
8.) the erosion rate remains approximately constant over a relevant time scale and
9.) the penetration depth scale of ^{10}Be is constant over a relevant time scale.

We set $N = N(t,z)$ which is equal to the concentration of ^{10}Be in soil at depth, z, and time, t and define $\int_{z(t)}^{0} N(t,z)dz$ as the total amount of ^{10}Be in soil at time t. [10]

We assume ^{10}Be decreases exponentially with depth [Eq. 2].

$$N(z,t) = N_{surf}(t)e^{-z*k} \quad [11]$$

Where $N_{surf}(t)$=^{10}Be concentration in the topsoil which may change as a function of time, and k is a constant describing the decrease of nuclides by adsorption at depth. Although this relationship may have exceptions over the scale of an entire watershed, small scale variations hopefully average-out over large watershed spatial scale which allows the application of the basin-wide approach in a basin a wide range of soil depths and adsorption length-scales. Equation [11] differs from equation [2] only in the way that N_{surf} is allowed to change with time. This equation implies that N_{surf} has an immediate effect on the ^{10}Be concentration in the whole soil column. This assumption works well in most cases where the percolation of ^{10}Be-laden rain into the soil is much faster than the erosion processes.

Thus $$I(t) = \int_{z_1}^{0} \rho N_{surf}(t) \exp[k(z(t) - 0)]dz \quad [12]$$

$$= N_{surf}(t)\frac{\rho}{k}\{1 - \exp[k(z_1(t) - 0)]\} \quad [13]$$

Let $s(t) = z_1(t) - 0$ be soil depth as a function of time thus,

$$I(t) = N_{surf}(t)\frac{\rho}{k}\left[1 - e^{-ks(t)}\right] \quad [14]$$

Assume constant soil depth, s(t) = s, according to assumption 7.

So $$I(t) = N_{surf}(t)\frac{\rho}{k}\left[1 - e^{-ks}\right] \quad [15]$$

Next, to solve the differential equation [5] and to eliminate the inventory I, which cannot be measured directly from river sediment, we substitute the right hand side of equation [15] for inventory in equation [5], separate the terms and solve over the same time scale for simultaneous loss through erosion, and loss through decay:

$$N'_{surf}(t)\frac{\rho}{k}\left[1-e^{-ks}\right]=-\lambda N_{surf}(t)\frac{\rho}{k}\left[1-e^{-ks}\right]-N_{surf}(t)\rho E(t)+Q). \quad [16]$$

By rearranging and solving for erosion rate E(t)

$$E(t)\rho=\frac{-\lambda N_{surf}(t)\frac{\rho}{k}\left[1-e^{-ks}\right]-N'_{surf}(t)\frac{\rho}{k}\left[1-e^{-ks}\right]+Q).}{N_{surf}(t)} \quad [17]$$

If nuclide steady-state has been reached, then $N_{surf}(t)$ is constant at all times t and $N_{surf}(t)= N_{surf}$ is constant. If this is the case, $N_{surf}'(t)=0$ and may be eliminated above such that

$$E(t)\rho=\frac{-\lambda N_{surf}\frac{\rho}{k}\left[1-e^{-ks}\right]+Q.}{N_{surf}} \quad [18]$$

$$E(t)=\frac{\lambda}{k}\left[1-e^{-ks}\right]-\frac{Q}{\rho N_{surf}}. \quad [19]$$

If E(t) is approximately constant or hovers around some average value over some time scale of integration, then

$$E=\frac{\lambda}{k}\left[1-e^{-ks}\right]-\frac{Q}{\rho N_{surf}} \quad [20]$$

and the erosion rate, E, can be calculated from a single sample of surface soil, N_{surf}. This equation has some only loosely-known parameters like soil depth and the decay constant that describes the downward migration of ^{10}Be into the soil. Over the scale of an entire watershed, these simplifying estimates can be made to evaluate the result of these unknowable parameters.

If the depth of the soil is large compared to the k term (s >> 1/k), the e^{-ks} term becomes insignificant. With increasing erosion rate, the concentration of ^{10}Be in the topsoil decreases and the decay term becomes increasingly insignificant ($\rho/k >> 1/\lambda$) (Fig. 11a). Estimates of the $\lambda/(\rho/k)$ term are very small (2×10^{-6} – 2×10^{-10}) for a full range of estimates for k (0.1-1000 cm) calculated based on ^{7}Be and ^{10}Be depth profile data (Blake et al., 1999, Pavich et al., 1986, 1993, 1997; Balco, 2004) in undisturbed soil and terraces. Thus, we can write:

$$E=\frac{Q}{\rho N_{surf}} \quad [21]$$

such that the erosion rate is roughly proportional to the local flux divided by the surface concentration. This equation also is easily derived from equation 5, if one assumes that the effect of decay is minimal. In this case of an exponential decrease of the ^{10}Be in a soil profile with increasing depth, the time to steady state can be approximated by dividing the attenuation length by the denudation rate. So for clay-rich soils that adsorb all the ^{10}Be in the upper parts of the soil with an attenuation length of 10 cm and an erosion rate of 100 mm ky^{-1}, the time to reach steady state (thus the averaging time scale) equals ~1000 yr. On the other hand, a coarse-grained soil may have an attenuation length of 50 cm and would average over ~5000 yr for the same erosion rate. For a lower erosion rate of 10 mm/ky and an attenuation length of 5 cm, the averaging time scale is closer to 10,000 yr.

We can now use equation [19] to evaluate the range of conditions over which erosion rates can be determined (Fig. 11a) At low erosion rates ^{10}Be is at secular equilibrium between the atmospheric flux Q and radioactive decay, and the concentration at the surface mainly depends on the depth of ^{10}Be percolation. At higher erosion rates a linear relationship between erosion rate and surface concentration results for most plausible depth settings. At low depths and shallow adsorption this linear range extends to erosion rates of 0.1mm ky^{-1}, while in typical tropical settings where soils are deep and Be penetrates deeply, the lowest possible erosion rate measurable is ca. 10 mm ky^{-1}. It is encouraging that, at steady state, for most plausible erosion rates the concentration does not depend on the depth scale which makes the cumbersome determination of inventories unnecessary. Inventories of ^{10}Be, however, may always be used in small sections to evaluate the retention behavior and 'attenuation' length-scale of individual soils.

Whether steady state has been achieved in a given environment can be estimated to a first order from the erosion rate and the ^{10}Be percolation depth. We simply assume that steady state is achieved after ca. 4-5 integration time scales have passed, and these can be roughly estimated by dividing the adsorption depth 1/k by the erosion rate (Fig. 11b). This calculation is similar to the *in situ* approach, but here the time scale also depends on the depth scale, which is variable. Roughly, the integration time scale increases by one order of magnitude for each order of magnitude increase in 1/k (Fig. 11b). Although the *in situ* ^{10}Be approach (with a fixed depth scale of 60 cm), integrates an erosion rate of 50 mm ky^{-1} over 12 ky, meteoric ^{10}Be penetrating to a depth of only 5 cm integrates over only 100 y (Fig. 11b). In deep soils with a 5 m ^{10}Be depth scale, a rate of 50mm ky^{-1} would integrate over 10^5 yr. Therefore, if the depth scale is shallow, the resolution of land use-related changes in erosion rate might become feasible, while with soils with deeply penetrating ^{10}Be a long-term time average erosion rate will be measured.

Bioturbation also exerts an additional complication for meteoric ^{10}Be. For *in situ*-produced ^{10}Be, bioturbation helps maintain the steady state concentration in the face of shallow episodic erosion (Granger et al., 1996). A similar result is possible with meteoric ^{10}Be provided that the depth of bioturbation is not greater than the depth of meteoric ^{10}Be penetration. With both systems, the time to steady state increases with greater bioturbation depth and can have a significant effect (e.g. doubling) on the time required to achieve steady state (Parker and Perg, 2005).

4. METHOD CAVEAT, FUTURE APPLICATIONS AND PREREQUISITES

We have shown that the flux of ^{10}Be is predictable for various geographic and climatic settings, and that where inventory measurements of ^{10}Be in precipitation records and in soils exist, these agree remarkably well with the predictions. Therefore, the measurement of meteoric ^{10}Be in soils can be used to measure the age and erosion rate of that soil. Landscapes are considered in steady state with respect to their cosmogenic meteoric ^{10}Be if the flux of meteoric fallout matches the flux of ^{10}Be adsorbed to the outside of particles that leave the system. Where meteoric ^{10}Be received by precipitation is retained on particles, this case is likely to exist. The environment where this requirement is most likely met is one in which the degree of water infiltration versus surface runoff is high, and where the pH in soils is > 6, so that both reactive $Be(OH)_2$ and organic Be complexes are mostly retained and are not competing with mobilized Al for adsorption sites. Fortunately, the steady-state assumption can be tested by measuring discrepancy between the flux of sediment-adsorbed ^{10}Be out of a basin and that entering the basin by meteoric deposition. To this end, the actual erosion rate can be independently measured with *in situ*-produced ^{10}Be in river-borne quartz. However, the time scale of integration of both systems is inherently linked to the depth scale of *in situ*-production with depth and erosion of that depth scale and meteoric ^{10}Be migration through the soil column. Fine-grained soils have shorter averaging time scales (decades to centuries) while coarse grained soils have longer averaging time scales (millennia). This potential diversity in possible depth-, and hence time scales over which the system operates offers opportunities, rather than presenting irresolvable obstacles. For example, should a long adsorption depth scale be identified for a given setting from soil depth profiles, then as in *in-situ* applications, erosion rates calculated for such a setting record a long-term average that is presumably unaffected by short-term anthropogenic effects (von Blanckenburg, 2005). If, on the other hand, the depth scale is shallow, not much time averaging will take place and the erosion rate possibly reflects an anthropogenic perturbation. On intermediate depth and hence temporal scales, the relationship between precipitation patterns and ensuing erosion rates might become resolvable. While much of these examples are possible on both the soil profile scale and the basin-wide scale, settings which would be

most likely candidates for this basin-wide erosion rate technique to succeed would be places where the soil is homogenous, the subsurface contains no impermeable layers, the drainage network is well-integrated and where the erosion rate is high. In places where these conditions are not met, it is possible that over the entire basin small perturbations in the direct, simple path of adsorbed ^{10}Be into the stream average out such that the condition is met.

Unfortunately, at this point, it is not possible to distinguish changes in adsorption depth from changes in erosion rate. Both systems would present themselves as only a concentration to then be interpreted with caution. Penetration depth could change with climate and vegetation, and also with land use. Problems also occur when the erosion process is itself excavates deep sediment. Like landsliding in steep, tectonically active terrains, agricultural impacts on the landscape may cause even more problems for the assumptions given above for a steady state landscape because of the large portion of the landscape that is affected. In this case, if soil is stripped rapidly over some depth interval greater than the adsoption depth over large portions of the landscape, then the assumptions in the steady state erosion model do not hold true. Specifically, the concentration in the stream sediment is no longer equal to the concentration at the ground surface, but instead is equal to the average over the stripped interval. Soil plowing however, may result in something akin to bioturbation and could protect the system in a steady state concentration if given sufficient time in the new agricultural regime.

We are likely to see a flurry of meteoric ^{10}Be applications and experiments on downward migration/percolation of ^{10}Be in the soil and meteoric-cosmogenic steady state of a watershed and basin-scale production rate refinement as well as newly possible applications. Potential applications (given ideal conditions for ^{10}Be retention) must be carefully chosen to avoid systems where the technique is not likely to work; these applications will revolve mainly around the following themes:

1. the ability to assign exposure ages to geomorphic surfaces and deposits with meteoric ^{10}Be where *in situ*-methods fail (e.g. Scherer et al., 1998; Lebatard et al., 2008).
2. an erosion rate meter and sediment tracer for geomorphic studies (e.g. L. Brown et al., 1988; You et al., 1988; McKean et al., 1993; Balco, 2004).

5. CONCLUSIONS

We have shown that many of the obstacles impairing the applicability of the meteoric ^{10}Be tracer in the early 1990s have in the meantime become tractable. We described:

1) a much better constrained numerical model quantifying global production and delivery of meteoric ^{10}Be;
2) the existence of numerous rain, ice core, soil, and lake sediment records that allow comparison of the theoretical predictions with those observed, and whose agreement is remarkable;
3) the observations from ice core records that variations of ^{10}Be flux as caused by solar modulation which may average out over the time scale of soil accumulation;
4) the finding that, in many settings, the cosmogenic nuclide flux ^{10}Be and ^{7}Be is independent of the rate of precipitation, making the assumption of a ^{10}Be flux that does not depend on knowing the rate of precipitation likely;
5) a better understanding of the retention of meteoric ^{10}Be during adsorption in soils and sediment, and more details for the speciation under which Be is likely to be retained;
6) the description of the grain size dependence on adsorption such that sediment and soil concentrations can be normalized to a uniform reference grain size;
7) an algebraic expression describing the steady state inventory of ^{10}Be from eroding surfaces.

This analysis shows that where erosion exceeds the time scale of steady state accumulation of ^{10}Be, the surface concentration is independent of the depth distribution of ^{10}Be in soils. This latter finding provides strong support for the suggestion that this tracer might, in the future, serve as powerful a tool as the *in situ*-produced cosmogenic nuclides to derive erosion rates and soil residence times from individual soil surface samples or detrital river sediment. However, the required effort for sample amounts, preparation, and analysis is far less than that of the *in situ* method. We suggest that experiments to better constrain the production, delivery, adsorption, depth percolation, and retention behavior on river particles of meteoric ^{10}Be would enable better age and erosion rate estimates in the future.

6. ACKNOWLEDGEMENTS

We acknowledge the support of German Science Foundation Grant *BL562/7*. JKW thanks the Alexander von Humboldt foundation for a postdoctoral fellowship. We had fruitful conversations Dirk Sachse and Peter Kubik. We also thank Jürg Beer, Christy Field and Jozef Masarik for generous data sharing. Finally, reviews by Peter Whiting, Darryl Granger, Marcus Christl and anonymous reviewers greatly improved the clarity and logic of the earlier version of this synthesis.

7. REFERENCES

Aldahan, A., Haiping, Y., Possnert, G. 1999. Distribution of beryllium between solution and minerals (biotite and albite) under atmospheric conditions and variable pH. Chemical Geology 156: 209-229.

Anderson, R.F., Lao, Y. Broecker, W.S. Trumbore, S.E. Hofmann, H.J. Wolfli, W. 1990. Boundary scavenging in the Pacific Ocean: a comparison of ^{10}Be and ^{231}Pa. Earth and Planetary Science Letters 96: 287-304.

Balco, G. 2004. The sedimentary record of subglacial erosion beneath the Laurentide Ice Sheet. Ph.D. Thesis University of Washington. 137 pp.

Bard, E., Raisbeck, G. M. Yiou, F. and Jouzel J. 1997. Solar modulation of cosmogenic nuclide production over the last millennium: Comparison between ^{14}C and ^{10}Be records. Earth and Planetary Science Letters 150: 453-462.

Barg, E. 1992. Studies of Beryllium geochemistry in soils: feasibility of using ^{10}Be/^{9}Be ratios for age determination. Ph.D thesis. University of California San Diego. 191 pp.

Barg, E., Lal, D., Pavich, M.J., Caffee, M.W., Southon, J.R. 1997. Beryllium geochemistry in soils: evaluation of ^{10}Be/^{9}Be ratios in authigenic minerals as a basis for age models. Chemical Geology 140: 237-258.

Baumgartner, S., Beer, J., Wagner, G., Kubik, P.W., Suter, M., Raisbeck, G.M., Yiou, F. 1997. ^{10}Be and dust. Nuclear Instruments and Methods B123: 296-301.

Beer, J., Siegenthaler, U., Bonani, G., Finkel, R.C., Oeschger, H., Suter, M., Wölfli, W. 1988. Information on past solar activity and geomagnetism from ^{10}Be in the Camp Century ice core. Nature 331: 675-679.

Beer, J. 2000. Long-term indirect indices of solar variability. Space Science Reviews 94: 53- 66.

Belmaker, R., Lazar, B., Tepelyakov, N., Stein, M., Beer, J. 2008. 10Be in Lake Lisan sediments - A proxy for production or climate? Earth and Planetary Science Letters 269(3-4): 447-456.

Berggren, D., Mulder, J. 1995. The role of organic matter in controlling aluminum solubility in acidic mineral horizons. Geochimica et Cosmochimica Acta 59**:** 4167-4180.

Bierman, P.R., Steig, E.J. 1996. Estimating rates of denudation using cosmogenic isotope abundances in sediment. Earth Surface Processes and Landforms 21: 125-139.

Blake, W.H., Walling, D.E., He, Q. 2002. Using cosmogenic beryllium-7 as a tracer in sediment budget investigations. Geografiska Annaler 84A: 89-102.

Bourlès, D., Raisbeck, G.M., Yiou, F. 1989. ^{10}Be and ^{9}Be in marine sediments and their potential for dating. Geochimica et Cosmochimica Acta 53: 443-452.

Brown, L., 1984. Applications of accelerator mass spectrometry. Annual Review of Earth and Planetary Sciences 12: 39-59.

Brown, L. 1987. ^{10}Be as a tracer of erosion and sediment transport. Chemical Geology 65: 189-196.

Brown, L. Pavic, M.J. Hickman, R.E. Klein, J. Middleton, R. 1988. Erosion of the Eastern United States observed with ^{10}Be. Earth Surface Processes and Landforms 13: 441-457.

Brown, L., Stensland, G.J., Klein, J., Middleton, R. 1989. Atmospheric deposition of ^{7}Be and ^{10}Be, Geochimica et Cosmochimica Acta 53: 135-142.

Brown, E.T., Edmond, J.M., Raisbeck., G.M. Bourlès, D., Yiou, F., Measures., C. 1992. Beryllium isotope geochemistry in tropical river basins. Geochimica Cosmochimica Acta 56: 1607-1624.

Chmeleff J., von Blanckenburg F., Kossert K., Jacob D., 2009. Determination of the ^{10}Be half-life by multicollector ICP-MS and liquid scintillation counting. Nuclear Instruments and Methods B: doi:10.1016/j.nimb.2009.09.012.

Cockburn, H.A.P., Summerfield M.A. 2004. Geomorphological applications of cosmogenic isotope analysis. Progress in Physical Geography 28: 1-42.

Deurer, M., Green, S.R., Clothier, B.E., Bottcher, J., Duijnisveld, W.H.M. 2003. Drainage networks in soils. A concept to describe bypass-flow pathways. Journal of Hydrology 272: 148-162.

EPICA Community Members. 2004. Eight glacial cycles from an Antarctic ice core. Nature 429: 623.

Feely, H.W., Larsen, R.J., Sanderson, C.G. 1989. Factors that cause seasonal variations in beryllium-7 concentrations in surface air. Journal of Environmental Radioactivity 9: 223–249.

Field, C.V., Schmidt, G.A., Koch, D., Salyk, C. 2006, Modeling production and climate-related impacts on ^{10}Be concentration in ice cores. Journal of Geophysical Research 111 (D15107) doi:10.1029/2005JD006410.

Finkel, R.C., Nishiizumi, K. 1997. Beryllium-10 concentrations in the Greenland Ice Sheet Project 2 ice core from 3–40 ka. Journal of Geophysical Research, C. Oceans 102: 26,699-26,706.

Frank, M., B. Schwarz, et al., 1997. A 200 kyr record of cosmogenic radionuclide production rate and geomagnetic field intensity from ^{10}Be in globally stacked deep-sea sediments. Earth and Planetary Science Letters 149: 121-129.

Frank, M., Backman, J., Jakobsson, M., Moran, K., O'Regan, M., King, J., Haley, B.A., Kubik, P.W. Garbe-Schönberg, D. 2008. Beryllium isotopes in central Arctic Ocean sediments over the past 12.3 million yr: Stratigraphic and paleoclimatic implications. Paleoceanography 23, PA1S02, doi:10.1029/2007PA001478.

Freeze, R.A., Cherry, J.A., 1979. Groundwater. Prentice-Hall. 604 pp.

Fuller, T.K., Perg, L.A., Willenbring, J.K., Lepper, K. 2009. Field evidence for climate-driven changes in sediment supply leading to strath terrace formation. Geology 37: 467-470.

Gosse, J.C. Phillips, F.M. 2001. Terrestrial in situ cosmogenic nuclides: theory and application, Quaternary Science Reviews 20: 1475- 1560.

Graham, I. Ditchburn, R., Barry, B. 2003. Atmospheric deposition of ^{7}Be and ^{10}Be in New Zealand rain (1996–98). Geochimica Cosmochimica Acta 67: 361-373.

Granger, D.E., Muzikar, P.F. 2001. Dating sediment burial with in situ-produced cosmogenic nuclides: theory, techniques, and limitations. Earth Planetary Science Letters 188: 269-281.

Granger, D.E., Kirchner, J.W., Finkel, R. 1996. Spatially averaged long-term erosion rates measured from in situ-produced cosmogenic nuclides in alluvial sediment. Journal of Geology 104: 249-257.

Gregg, S.J., Sing, K.S.W. 1982. Adsorption, Surface Area and Porosity. Academic Press.303 pp.

Gu, Z.Y., Lal, D., Liu, T.S., Southon, J., Caffee, M.W., Guo, Z.T., Chen, M.Y. 1996. Five million year ^{10}Be record in Chinese loess and red clay: climate and weathering relationships, Earth Planetary Science Letters 144: 273-287.

Gustafsson, J.P., Pechová, P., Berggren, D. 2003. Modelling metal binding to soils: The role of organic matter. Environmental Science and Technology 37: 2767-2774.

Hawley, N., Robbins, J.A., Eadie, B.J. 1986. The partitioning of 7-beryllium in fresh water. Geochimica Cosmochimica Acta 50: 1127-1131.

He, Q., Walling, D.E. 1996. Use of fallout Pb-210 measurements to investigate longer-term rates and patterns of overbank sediment deposition on the floodplains of lowland rivers. Earth Surf. Processes and Landforms 21: 141-154.

Heikkilä, U., Beer, J. and Alfimov, V. 2008. Beryllium-10 and Beryllium-7 in precipitation in Dübendorf (440 m) and at Jungfraujoch (3580 m), Switzerland (1998-2005). Journal of Geophysical Research 113: D11104, doi: 10.1029/2007JD009160.

Heikkilä, U. 2007. Modeling of the atmospheric transport of the cosmogenic radionuclides ^{10}Be and ^{7}Be using the ECHAM5-HAM General Circulation Model. Ph.D. thesis. ETH-Zurich. 148 pp.

Helz, G.R., Valette-Silver, N. 1992. Beryllium-10 in Chesapeake Bay sediments: an indicator of sediment provenance. Estuarine, Coastal and Shelf Science 34: 459-469.

Jickells, T.D., An, Z.S., Andersen, K.K., Baker, A.R., Bergametti, G., Brooks, N., Cao, J.J., Boyd, P.W., Duce, R.A., Hunter, K.A., Kawahata, H., Kubilay, N., laRoche, J. Liss, P.S., Mahowald, N., Prospero, J.M., Ridgwell,A.J., Tegen,I., Torres, R. 2005. Global Iron Connections between Desert Dust, Ocean Biogeochemistry, and Climate. Science 308: 67-71.

Kaste, J.M., Norton, S.A., Hess, C.T. 2002. Environmental chemistry of Beryllium-7. Reviews in Mineral Geochemistry 50: 271-289.

Keilen, K., Stahr, K., Goltz, H.v.d., Zöttl, H.W. 1977. Zur Pedochemie des Berylliums – Untersuchen einer Bodengesellschaft im Gebiet des Bärhaldegranits (Südschwarzwald). Geoderma 17: 315-329.

Knies, D. L., Elmore, D., Sharma, P., Vogt, S., Li, R., Lipschutz, M. E., Petty, G., Farrell, J., Yr, M. C., Fritz, S., Agee, E. 1994. ^{7}Be, ^{10}Be and ^{36}Cl in precipitation, Nuclear Instrument Methods Physics Research. B 92: 340-344.

Kollár, D., Leya, I., Masarik, J., Michel, R. 2000. Calculation of cosmogenic nuclide production rates in Earth's atmosphere and in terrestrial surface rocks using improved neutron cross sections. Meteoritics and Planetary Science 35: A90-A91.

Korschinek, G., Bergmaier, A., Faestermann, T., Gerstmann, U.C., Knie, K., Rugel, G., Wallner, A., Dillmann, I., Dollinger, G., Lierse von Gostomskie, C., Kossert, K., Maitia, M., Poutivtsev, M., Remmert, A. 2009. A new value for the half-life of ^{10}Be by heavy ion elastic recoil detection and liquid scintillation counting Nuclear Instruments and Methods B: doi:10.1016/j.nimb.2009.09.020.

Kretzschmar, R., Robarge, W.P., Amoozegar, A. 1995. Influence of natural organic matter on colloid transport through saprolite. Water Resources Research 31: 435-445.

Lal, D. 1987. ^{10}Be in polar ice: Data reflect changes in cosmic ray flux or polar meteorology. Geophysical Research Letters 14: 785-788.

Lal, D. 1991. Cosmic ray labeling of erosion surfaces: in situ nuclide production rates and erosion models. Earth and Planetary Science Letters 104: 424- 439.

Lal, D., 1999. New Nuclear Methods for Studies of Soil Dynamics Utilizing Cosmic Ray Produced Radionuclides Pages 1044-1052 In: D.E. Stott, R.H. Mohtar and G.C. Steinhardt (eds). 2001. Sustaining the Global Farm. Selected papers from the 10th International Soil Conservation Organization Meeting held May 24-29, 1999 at Purdue University and the USDA-ARS National Soil Erosion Research Laboratory.

Lal, D. 2007. Recycling of cosmogenic nuclides after their removal from the atmosphere; special case of appreciable transport of ^{10}Be to polar regions by aeolian dust. Earth and Planetary Science Letters 264: 177-187.

Lal, D., Peters, B. 1967. Cosmic rays produced radioactivity on the Earth. In: K. Site, Editor, Handbuch der Physik, Springer-Verlag, New York. 551-612.

Lebatard, A.-E., Bourlès, D., Duringer, P., Jolivet M., Braucher R., Carcaillet J., Schuster, M., Arnaud, N., Monié, P., Lihoreau, F. Likius, A., Mackaye, H.T., Vignaud, P., Brunet, M. 2008. Cosmogenic nuclide dating of Sahelanthropus Tchadensis and Australopithecus bahrelghazali: Mio-Pliocene hominids from Chad. Proceedings of the National Academy of Sciences 105: 3226-3231.

Ljung, K., Björck, S, Muscheler, R., Beer, J., Kubik, P.W. 2007. Variable ^{10}Be fluxes in lacustrine sediments from Tristan de Cunha, South Atlantic: a solar record? Quaternary Science Reviews 26: 829-835

Lundberg, L., Ticich, T., Herzog, G. F., Hughes, T., Ashley, G., Moniot, R. K., Tuniz, C., Kruse, T. and Savin, W. 1983. ^{10}Be and Be in the Maurice River-Union Lakes system of Southern New Jersey. Journal of Geophysical Research 88: 4498-4504.

Maejima Y., Matsuzaki H., Higashi T. 2005. Application of cosmogenic ^{10}Be to dating soils on the raised coral reef terraces of Kikai Island, southwest Japan. Geoderma 126: 389-399.

Masarik, J., Reedy, R.C. 1995. Terrestrial cosmogenic-nuclide production systematics calculated from numerical simulations. Earth Planetary Science Letters 136: 381– 395.

Masarik, J., Beer, J. 1999. Simulation of particle fluxes and cosmogenic nuclide production in the Earth's atmosphere. Journal of Geophysical Research 104: 12,099-12,111.

Masarik J., Beer, J. 2009. An updated simulation of particle fluxes and cosmogenic nuclide production in the Earth's atmosphere. Journal of Geophysical Research 114, D11103, doi:10.1029/2008JD010557.

McCracken, K.G. 2004. Geomagnetic and atmospheric effects upon the cosmogenic ^{10}Be observed in polar ice, Journal of Geophysical Research 109: A04101, doi:10.1029/2003JA010060.

McCracken, K.G., McDonald, F.B., Beer, J., Raisbeck, G., Yiou., F. 2004. A phenomenological study of the long-term cosmic ray modulation, 850 – 1958 AD, Journal of Geophysical Research 109: A12103, doi:10.1029/ 2004JA010685.

McHargue, L.R., Damon, P.E. 1991. The global beryllium-10 cycle, Reviews in Geophysics 29: 141-158.

McKean, J.A., Dietrich, W.E., Finkel, R.C., Southon, J.R., Caffee, M.W. 1993. Quantification of soil production and downslope creep rates from cosmogenic ^{10}Be accumulations on a hillslope profile. Geology 21: 343-346.

Meehan, W.R., Smythe, L.E. 1967. Occurrence of beryllium as a trace element in environmental materials. Environmental Science Techniques 1: 839-844.

Mitchell, T.D., Jones, R.G. 2005. An improved method of constructing a database of monthly climate observations and associated high-resolution grids. International Journal of Climatology 25: 693 – 712. DOI:10.1002/joc.1181

Monaghan, M.C. 1986. The global-average production rate of ^{10}Be, Earth and Planetary Science Letters 76: 279-287.

Monaghan, M.C., Krishnaswami, S., Thomas, J.H. 1983. ^{10}Be concentrations and the long term fate of particle-reactive nuclides in five soil profiles from California. Earth and Planetary Science Letters 65: 51-60.

Monaghan, M.C., McKean, J., Dietrich, W., Klein, J. 1992. ^{10}Be chronometry of bedrock-to-soil conversion rates. Earth and Planetary Science Letters 111: 483-492.

Muscheler, R., Beer, J., Wagner, G., Finkel, R.C. 2000. Changes in deep-water formation during the Younger Dryas event inferred from ^{10}Be and ^{14}C records. Nature 408: 567–70.

Muscheler, R., Beer, J., Kubik, P.W., Synal, H.A. 2005. Geomagnetic filed intensity during the last 60,000 yr based on ^{10}Be and ^{36}Cl from the Summit ice cores and ^{14}C. Quaternary Science Reviews 24: 1849-1860.

Nishiizumi, K., Winterer, E.L. Kohl, C.P. Klein, J. Middleton, R. Lal, D., Arnold, J.R. 1989. Cosmic ray production rates of ^{26}Al and ^{10}Be in quartz from glacially polished rocks. Journal Geophysical Research 94: 17907-17915.

Nishiizumi K., Imamura M., Caffee M.W., Southon J.R., Finkel R.C., McAninch J. 2007. Absolute calibration of ^{10}Be AMS standards. Nuclear Instruments Methods in Physics Research B 258: 403-413.

Nishiizumi, K., Welten, K.C., Matsumura, H., Caffee, M.C., Ninomiya, K., Omoto, T., Nakagaki, R., Shima, T., Takahashi, N., Sekimoto, S., Yashima, H., Shibata, S., Bajo, K., Nagao, K., Kinoshita, N., Imamura, M., Sisterson, J., Shinohara, A. 2009. Measurements of High-Energy Neutron Cross Sections for Accurate Cosmogenic Nuclide Production Rates. Geochimica Cosmochimica Acta Abstract A945.

Parker, G., Perg, L.A. 2005. Probabilistic formulation of conservation of cosmogenic nuclides: effect of surface elevation fluctuations on approach to steady state. Earth Surface Processes and Landforms 30: 1127-1144.

Pavich, M.J., Vidic, N. 1993. Application of paleomagnetic and ^{10}Be analyses to chronostratigraphy of Alpine glacio-fluvial terraces, Sara river valley, Slovenia. In: Swart, P. (Ed.), Climate Change in Continental Isotopic Records. AGU Geophysical Monographs 78: 263-275.

Pavich, M.J., Brown, L., Klein, J., Middleton, R. 1984. ^{10}Be accumulation in a soil chronosequence. Earth Planetary Science Letters 68: 198-204.

Pavich, M.J., Brown, L., Valette-Silver, N.J., Klein, J. and Middleton, R. 1985. ^{10}Be analysis of a Quaternary weathering profile in the Virginia Piedmont. Geology 13: 39-41.

Pavich, M.J., Brown, L., Harden, J., Klein, J., Middleton, R. 1986. ^{10}Be distribution in soils from Merced River terraces, California. Geochimica Cosmochimica Acta 50**:** 1727-1735.

Prospero, J.M. 1999. Long range transport of mineral dust in the global atmosphere: Impact of African dust on the environment of the southern United States. Proceedings of the National Academies of Science 96**:** 3396-3403.

Raisbeck G.M. et al. 1981. Cosmogenic ^{10}Be/^{7}Be as a probe of atmospheric transport processes. Geophysical Research Letters 8: 1015-1018.

Raisbeck, G. M., Yiou, F., Lieuvin, M., Ravel, J. C., Fruneau, M., et al. 1981c. 10Be in the environment : some recent results and their applications. Proc. Syrup. Accel. Mass Spectrom. Argonne, II1: Argonne Natl. Lab. 458 pp.

Reedy R.C. Predicting the production rates of cosmogenic nuclides. 2000. Nuclear Instruments and Methods in Physics Research, Section B: Beam Interactions with Materials and Atoms 172: 782-785.

Schaller, M., von Blanckenburg, F., Veldkamp, A., Tebbens, L.A., Hovious, N., Kubik, P.W. 2002. A 30 000 yr record of erosion rates from cosmogenic ^{10}Be in Middle European river terraces. Earth and Planetary Science Letters 204: 307-320.

Scherer, R.P., Aldahan, A., Tulaczyk, S., Possnert, G., Engelhardt, H., Kamb, B. 1998. Pleistocene Collapse of the West Antarctic Ice Sheet. Science 281: 82 – 85.

Segl, M., Mangini, A., Beer, J., Bonani, G., Suter, M., Wölfli, W. 1989. Growth rate variations of manganese nodules and crusts induced by paleoceanographic events. Paleoceanography 4: 511-530.

Shen, C.D., Beer, J., Liu, T.S., Oescheger, H., Bonani, G., Suter, M., Wölfli, W. 1992. ^{10}Be in Chinese loess. Earth Planetary Science Letters 109: 169-177.

Shen, C., Beer, J. Kubik, P.W., Suter, M., Borkovec, M., Liu, T.S. 2004. Grain size distribution, ^{10}Be content and magnetic susceptibility of micrometer–nanometer loess materials, Nuclear Instruments and Methods in Physics Research B 223–224: 613–617.

Staiger J.W., Gosse, J., Toracinta, R., Oglesby, B., Fastook, J., Johnson, J.V. 2007. Atmospheric scaling of cosmogenic nuclide production: Climate effect. Journal of Geophysical Research- Solid Earth 112: B02205, doi:10.1029/2005JB003811.

Steig, E.J., Polissar, P.J. Stuiver, M. Grootes, P.M., Finkel, R.C. 1996. Large amplitude solar modulation cycles of ^{10}Be in Antarctica: Implications for atmospheric mixing processes and interpretation of the ice core record. Geophysical Research Letters 23: 523–526.

Sugden, D.E., McCulloch, R.D., Bory, A. J.-M., Hein, A.S. 2009. Influence of Patagonian glaciers on Antarctic dust deposition during the last glacial period. Nature Geoscience 2, 281-285.

Summerfield, M.A., Hulton, N.J. 1994. Natural controls of fluvial denudation rates in major world drainage basins. Journal of Geophysical Research 99: 13871-13883.

Takahashi,Y., Minai, Y., Ambe, S., Makide,Y., Ambe, F. 1999. Comparison of adsorption behavior of multiple inorganic ions on kaolinite and silica in the presence of humic acid using the multitracer technique Geochimica et Cosmochimica Acta 63 (6): 815-836.

Thompson, A., Chadwick, O. Bowman, S. Chorover, J., 2006. Colloid Mobilization During Soil Iron Redox Oscillations. Environmental Science Technology 40: 5743-5749.

Usoskin, I.G., Solanki, S.K., Schüssler, M., Mursula, K., Alanko, K. 2003. Millennium-scale sunspot number reconstruction: Evidence for an unusually active sun since the 1940s. Physical Review Letters 91: 211101-1–211101-4.

Valette-Silver, J.N., Brown, L., Pavich, M., Klein, J., Middleton, R. 1986. Detection of erosion events using ^{10}Be profiles: Example of the impact of agriculture on soil erosion in the Chesapeake Bay Area. Earth and Planetary Science Letters 80: 82-90.

van Geen, A., Valette-Silver, N.J., Luoma, S.N., Fuller, C.C., Baskaran, M., Tera, F., Klein, J.. 1999. Constraints on the sedimentation history of San Francisco Bay from C-14 and Be-10. Marine Chemistry 64: 29-38.

von Blanckenburg, F. 2005. The control mechanisms of erosion and weathering at basin scale from cosmogenic nuclides in river sediment. Earth and Planetary Science Letters 237: 462-479.

von Blanckenburg, F., O'Nions, R.K., Belshaw, N.S., Gibb, A., Hein, J.R. 1996. Global distribution of Beryllium isotopes in deep ocean water as derived from Fe-Mn crusts. Earth and Planetary Science Letters 141: 213-226.

Vonmoos, M., Beer, J., Muscheler, R. 2006. Large variations in Holocene solar activity: Constraints from ^{10}Be in the Greenland Ice Core Project ice core. Journal of Geophysical Research 111: A10105 doi:10.1029/2005JA011500.

Wagner, G., Masarik, J., Beer, J., Baumgartner, S. Imobden, D., Kubik, P.W. Synal, H.A., Suter, M. 2000. Reconstruction of the geomagnetic field between 20 and 60 kyr BP from cosmogenic radionuclides in the GRIP ice core. Nuclear Instruments and Methods in Physics Research, Section B: Beam Interactions with Materials and Atoms 172: 597-604.

Wagner, G., Beer, J., Masarik, J., Muscheler, R., Kubik, P.W., Mende, W., Laj, C., Raisbeck, G.M., Yiou. F. 2001. Presence of the solar de Vries cycle (~205 yr) during the last ice age. Geophysical Research Letters 28: 303-306.

Wallbrink, P.J., Murray, A.S. 1994. Fallout of ^{7}Be in south eastern Australia. Journal of Environmental Radioactivity 25:213-228.

Wallbrink, P.J., Murray, A.S. 1996. Distribution and variability of ^{7}Be in soils under different surface cover conditions and its potential for describing soil redistribution processes. Water Resources Research 32: 467-476.

Webber, W. R., Higbie. P.R. 2003. Production of cosmogenic Be nuclei in the Earth's atmosphere by cosmic rays: Its dependence on solar modulation and the interstellar cosmic ray spectrum, Journal of Geophysical Research, A: Space Physics 108: 1355, doi:10.1029/2003JA009863.

Webber, W.R.. Higbie, P.R., McCracken. K.G. 2007. Production of the cosmogenic isotopes ^{3}H, ^{7}Be, ^{10}Be, and ^{36}Cl in the Earth's atmosphere by solar and galactic cosmic rays, Journal of Geophysical Research 112: A10106, doi:10.1029/2007JA012499.

Winckler,G. Anderson, R.F., Fleisher, M.Q., McGee, D., Mahowald, N. 2008. Covariant Glacial-Interglacial Dust Fluxes in the Equatorial Pacific and Antarctica. Science 320: 93-96.

Yiou, F., Raisbeck, G.M., Baumgartner, S., Beer, J., Hammer, C., Johnsen, S., Jouzel, J., Kubik, P.W., Lestringuez, J., Stiévenard, M., Suter, M., Yiou, P. 1997. Beryllium-10 in the Greenland Ice core at Summit, Greenland. Journal of Geophysical Research 102: 26,783-26,794.

Yiou, F., et al., 2002. GRIP Ice Core Beryllium 10 Data, IGBP PAGES/World Data Center for Paleoclimatology Data Contribution Series #2002-085. NOAA/NGDC Paleoclimatology Program, Boulder CO, USA.

You,.C.-F. Lee, T. Brown, L., Shen., J.J., Chen, J.-C. 1988. ^{10}Be study of rapid erosion in Taiwan. Geochimica Cosmochimica Acta 52: 2687-2691.

You, C.-F., Lee, T., Li, Y.H. 1989. The partition of Be between soil and water. Chemical Geology 77: 105-118.

Zhou, W., Priller, A., Beck, J.W., Zhengkun, W., Maobai, C., Zhisheng, A., Kutschera, W., Feng, X., Huagui, Y., Lin, L., 2007. Disentangling geomagnetic and precipitation signals in an 80-kyr Chinese loess record of ^{10}Be. Radiocarbon 49: 139-160.

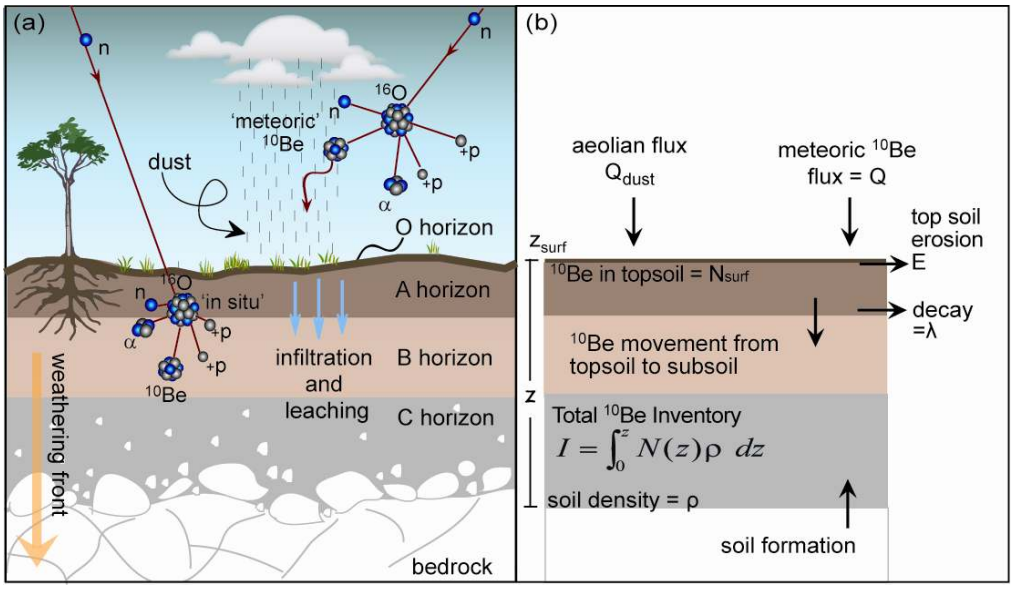

Figure 1: a.) Schematic diagram of a soil profile and the ways in which ^{10}Be can become incorporated into the soil. The weathering front follows the downward movement of percolating water from surface precipitation and (not shown) ground water.
b.) Schematic diagram of a soil profile and definitions of variables in Eq. 4-21.

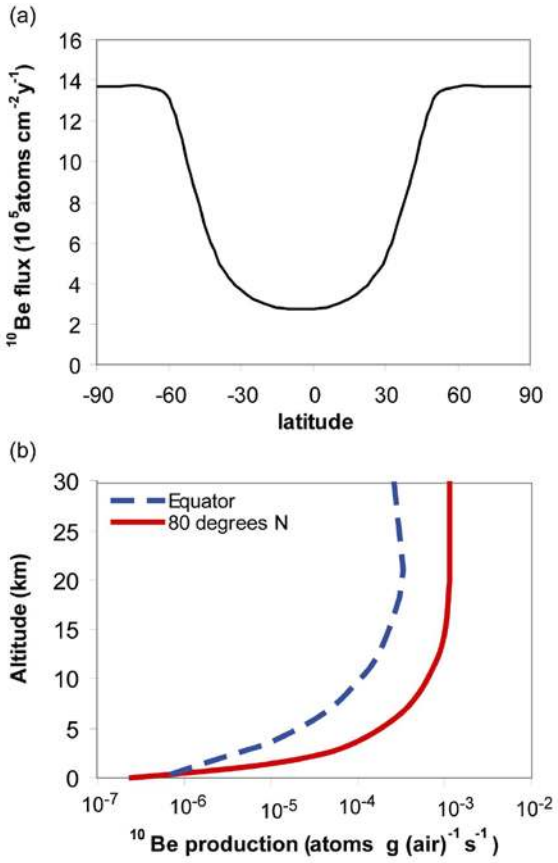

Figure 2: a.) Depth integrated ^{10}Be production rate of ^{10}Be for sea level by latitude from Masarik and Beer (1999) for long-term solar modulation (ϕ= 550 MeV) and present geomagnetic field intensity.
b.) The ^{10}Be production per gram of air as a function of altitude for 80°N and 0° latitude from Masarik and Beer (1999) for long-term solar modulation (ϕ= 550 MeV) and present geomagnetic field intensity translated to altitude using data from Staiger et al. (2007). Note that ca. 99% of the ^{10}Be is produced at altitudes > 3 km. Therefore, flux to the Earths surface without atmospheric transport or mixing (which is simply the production integrated over altitude) is independent of altitude for most geographic settings.

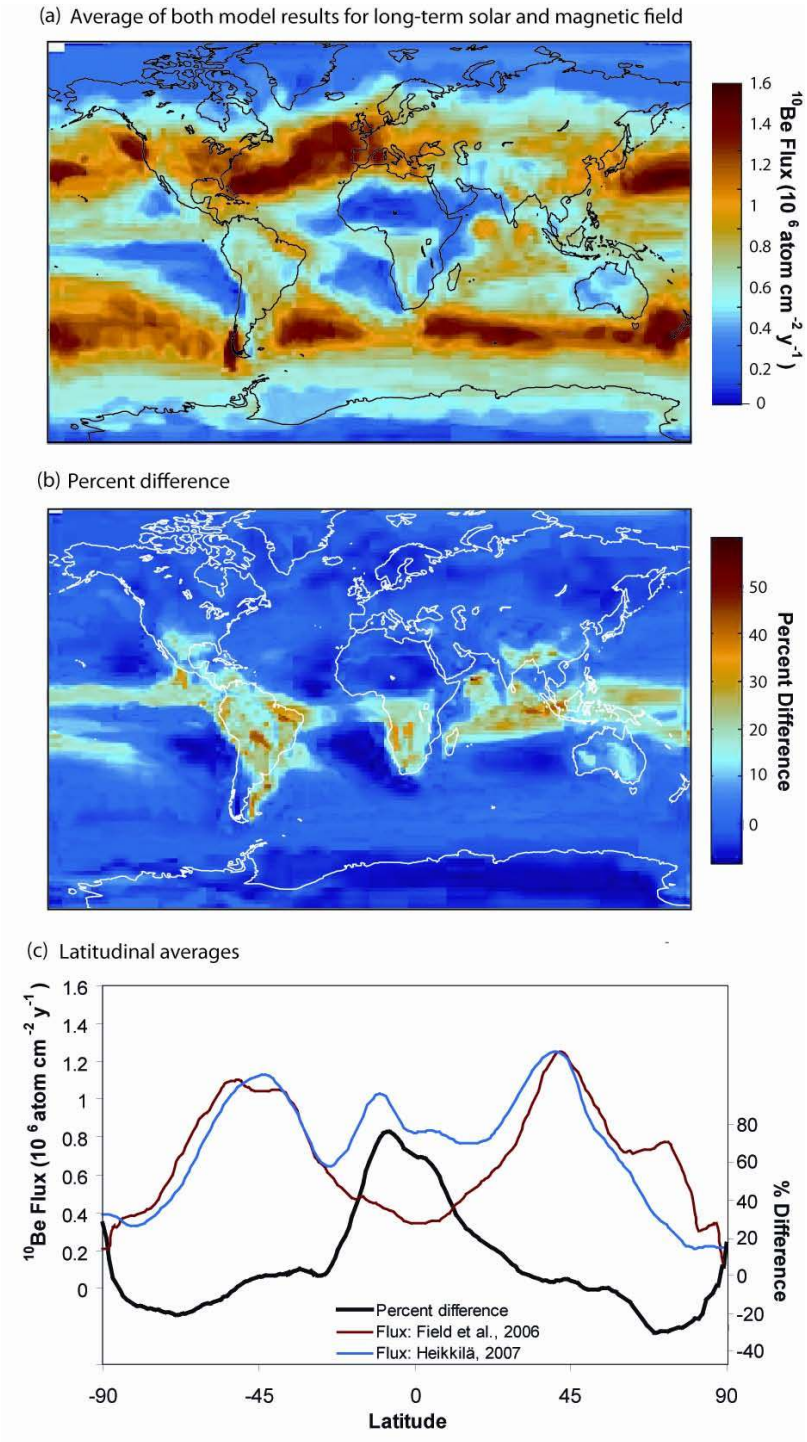

Figure 3: a.) Average ^{10}Be flux adapted from Heikkilä (2007) and Field et al. (2006), but for the long-term solar modulation factor and long-term geomagnetic field. The data was recalculated for each latitude using figure 5 of Field et al. (2006).
b.) The percentage difference ^{10}Be flux between the two models (calculated from Heikkilä, 2007 and Field et al., 2006).
c.) The latitudinally averaged flux for Heikkilä (2007) and Field et al. (2006) and the percentage difference ^{10}Be flux between the two models (calculated from Heikilä, 2007 and Field et al., 2006).

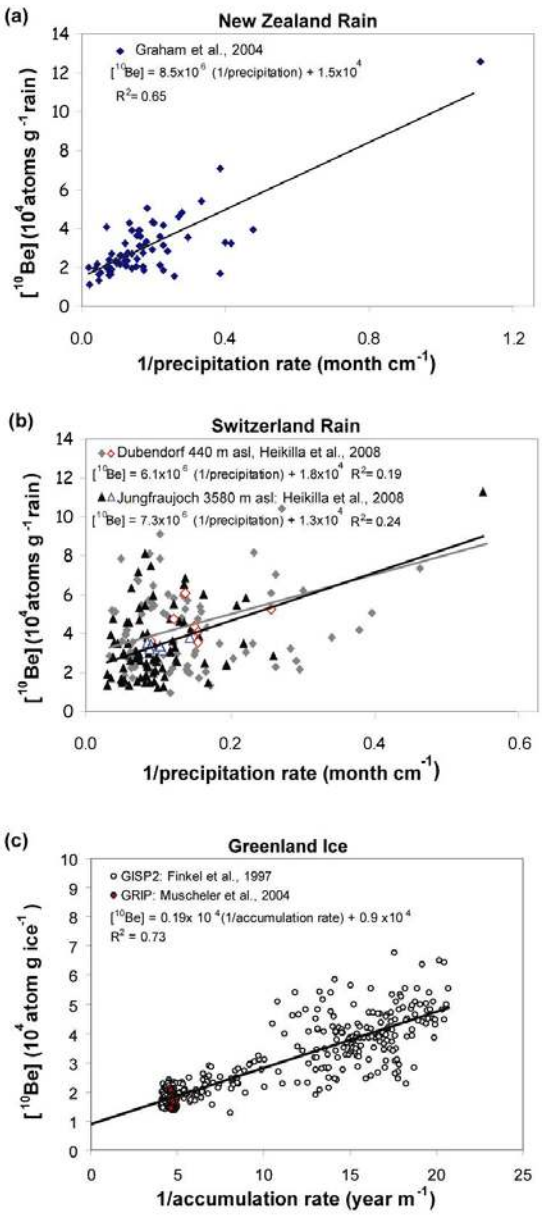

Figure 4: a.) ^{10}Be concentration in rain measured over 2 yr for New Zealand sites - all of which are located around 35-48 deg. latitude - versus the inverse of precipitation rate. The black line is the best fit line with a slope equal to the flux of ^{10}Be.
b.) ^{10}Be concentration in rain measured over 4 yr for Switzerland sites - all of which are located around 47 deg. latitude - versus the inverse of precipitation rate. The black and gray lines are the best fit lines with a slope equal to the flux of ^{10}Be. The hollow data points are concentrations and precipitation averaged over one year and renormalized for monthly precipitation. The yearly variability would be the variability closer to that seen in soils whose formation time averages over millennia. These datasets show a very similar flux even though the site altitudes differ by 3000 m.
c.) ^{10}Be concentration measured in ice through time in the GISP2 and GRIP ice cores versus the inverse of ice accumulation rate. The slope of the best fit line is similar to the predicted ^{10}Be flux. The y-intercepts of 4a-c provide the concentration of an initial uniform ^{10}Be load in precipitation; they match best estimates of the concentration of dust into the area.

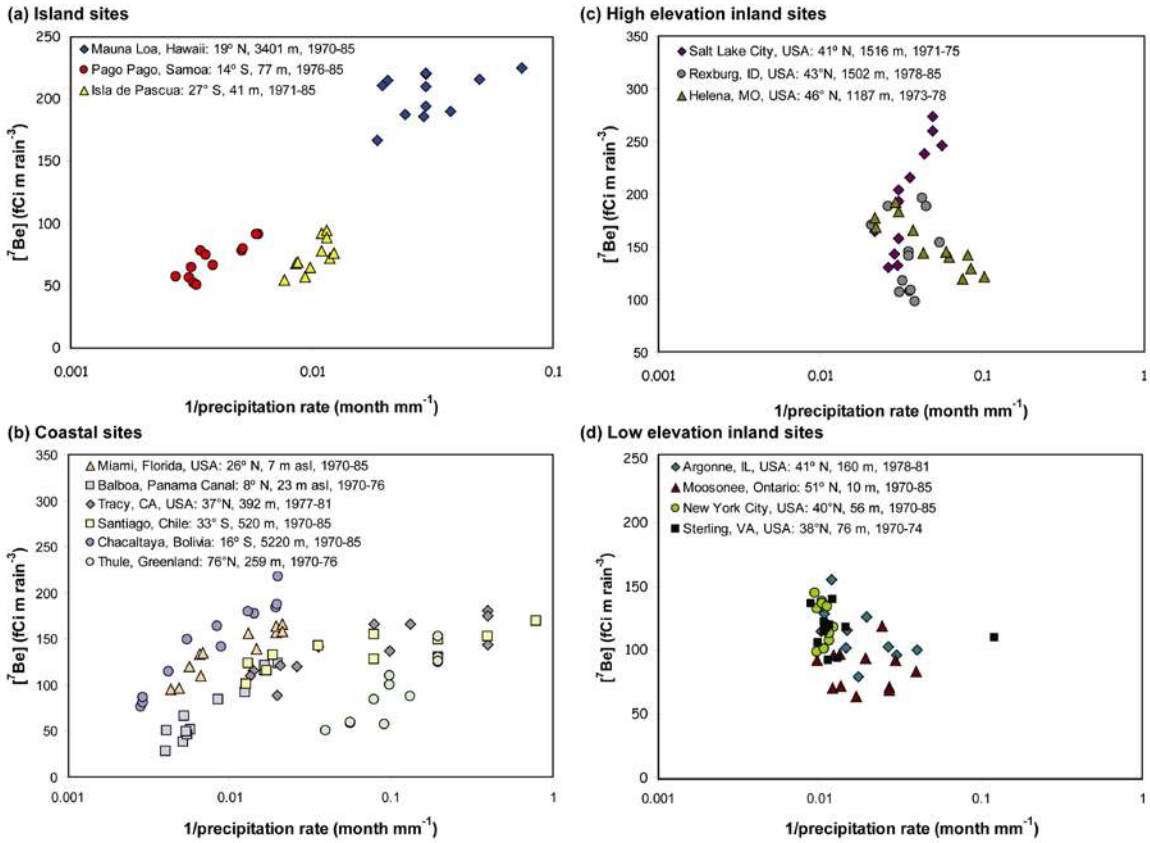

Figure 5: ^{7}Be concentration-inverse precipitation relationship for convective storm areas for a.) islands and b.) coastal settings. ^{7}Be concentration- inverse precipitation relationship for advective storm areas for c.) high elevation and d.) low elevation continental settings. ^{7}Be data are from Feely et al. (1989) and precipitation rates for the yr of sampling are from Mitchell and Jones (2005) and http://www.sws.uiuc.edu/data/climatedb/data.asp; Accessed June 14, 2008.

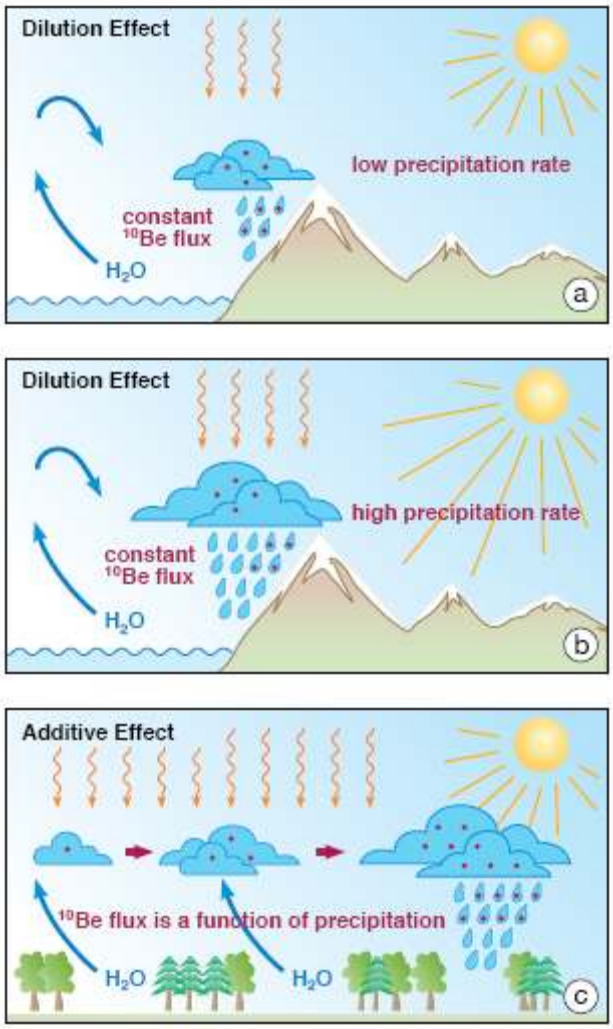

Figure 6: a.) Meteoric ^{10}Be (or ^{7}Be) fluxes from convective precipitation produce a 'dilution' effect. Here the cloud turnover rate is high and the cloud forms near where the rain falls then the total cosmogenic ^{10}Be flux for the year to a site is independent of the rate of precipitation.
b.) Same as in (a) but for high rates of precipitation. Note the number of ^{10}Be atoms precipitated (red dots) is the same as in case (a), but the atoms are diluted by more rain water.
c.) Advective clouds bring increasing fluxes of ^{7}Be (or ^{10}Be) with increasing amounts (and rates) of precipitation, thereby producing the "additive" effect.

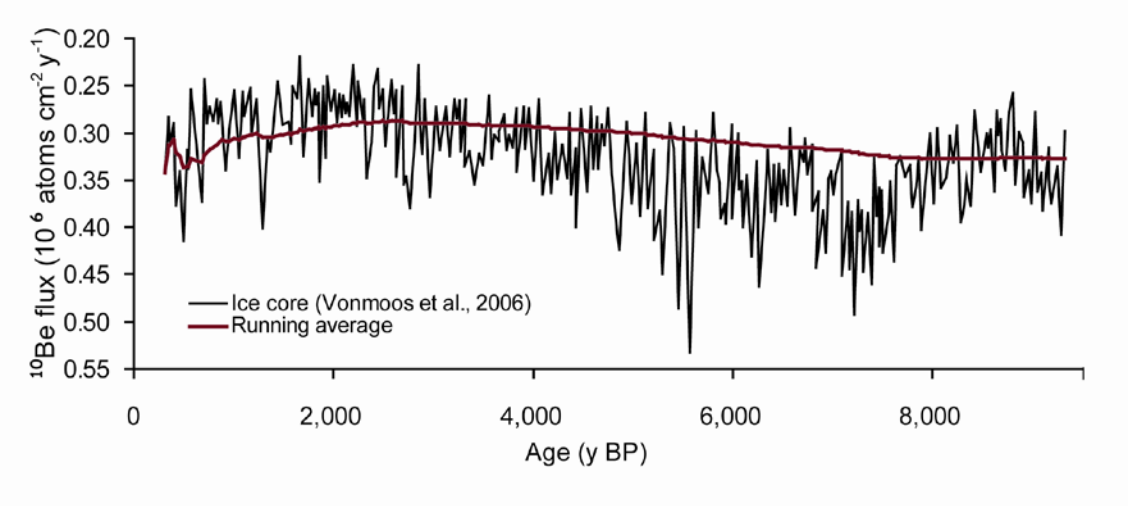

Figure 7: Measured flux of ^{10}Be through time (from Vonmoos et al., 2006) in the GRIP ice core. The integrated average smooths the observed variation due to changes in solar activity Φ to a quasi-permanent long-term average value similar to that expected from Heikkilä, 2007; and Field et al., 2006 when averaged over thousands of yr (see also Table 1). As soils accumulate over similar periods, we expect that variations in the flux of ^{10}Be are averaged out in a similar manner.

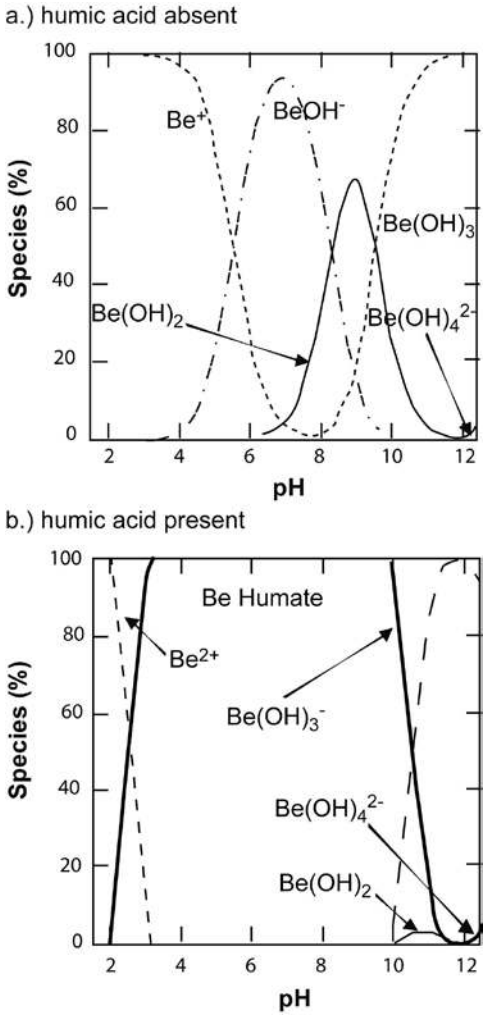

Figure 8: Be species in aqueous solutions from Takahashi et al. (1999). The concentration of solutes is assumed to be 0.02 M. a.) This graph shows Be speciation in the absence of humic acid b.) This graph shows the speciation in the presence of 30 mg/l humic acid.

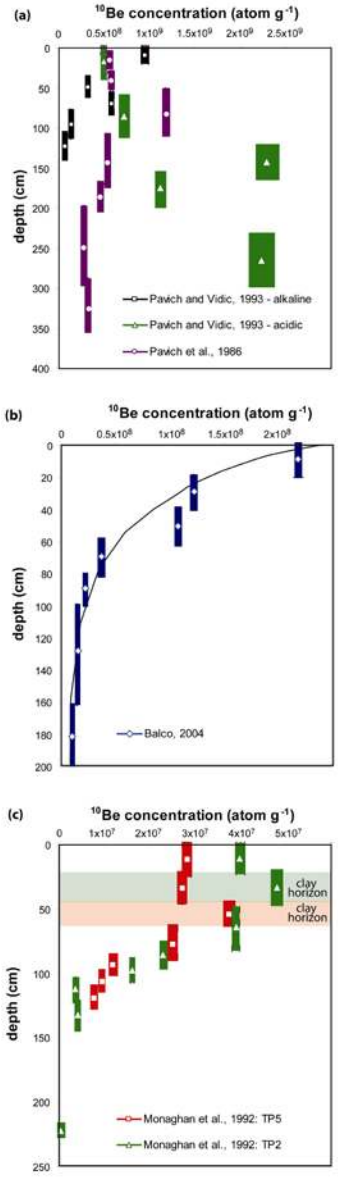

Figure 9: a.) A depth profile of meteoric ^{10}Be measured in an old Yugoslavian soil profile (Pavich et al., 1986)(purple) and in ~1.8-3 million-year-old soils from the Virginia Piedmont (green and black). The mobility of the meteoric cosmogenic ^{10}Be to greater depths reflects the pH of the soil as well as the age. In acidic soils (in green), the ^{10}Be concentration lacks a clear depth dependency (Pavich and Vidic, 1993). In younger alkaline soils (orange), the concentration decreases simply with depth with the exception of a mid-depth clay horizon which contains an anomalous surface area:mass ratio.
b.) A depth profile of meteoric ^{10}Be concentration measured in a late-glacial soil in Minnesota (Balco, 2004) can be used to calculate the mean soil residence time and to calibrate the exponential decrease of meteoric ^{10}Be with depth (best-fit black line). This profile has a 1/k depth of ~45 cm.
c.) Depth profiles of meteoric ^{10}Be measured in a soil in Black Diamond Mines Regional Park, Contra Costa County, California (Monaghan et al., 1992) showing an overall decrease with depth and a mid-depth maximum reflecting grain size effects. 1/k depths here range from 55-65 cm.

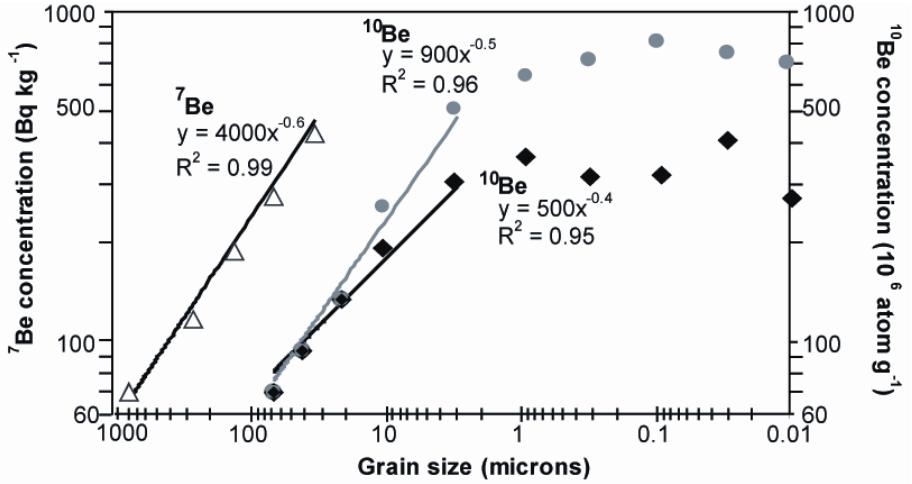

Figure 10: Grain-size dependency of the ^{7}Be (open triangles) in soil and ^{10}Be concentrations in soil (gray circles) and loess deposits (black diamonds). The power-law exponent that describes the steepest part of the function relating grain-size and nuclide concentrations has a value of -0.5 +/-0.1. ^{7}Be data is from soil plot experiments in Wallbrink and Murray (1994) and ^{10}Be data is from Shen et al. (2004). The smallest clays seem to have approximately equal concentrations.

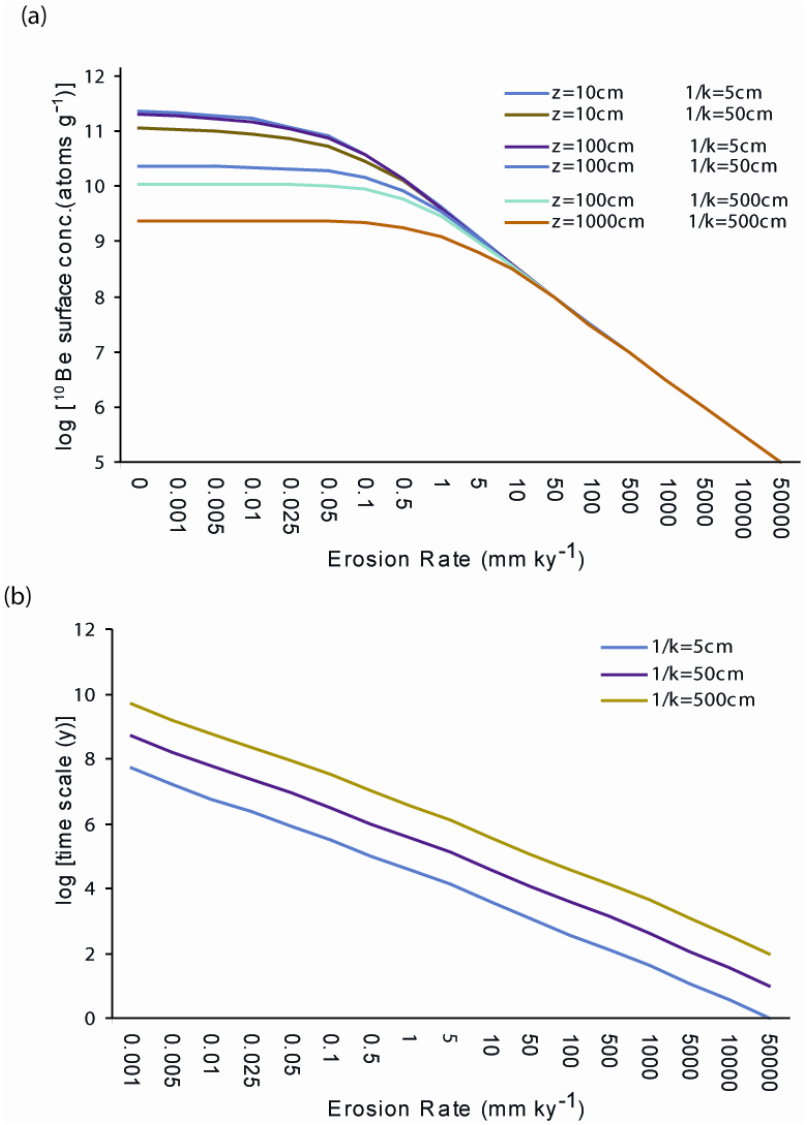

Figure 11: a.) Relationship between erosion rate and the concentration of ^{10}Be measured at the surface of a landscape or soil for a variety of typical soil depths z and adsorption depths 1/k (equation 19). The atmospheric flux Q was set to be 1×10^6 atoms cm^{-2} yr^{-1}, the half life of ^{10}Be at 1.39 My, and the density ρ at 2g cm^{-3}. At low erosion rates, ^{10}Be is at secular equilibrium between atmospheric flux Q and radioactive decay. At higher erosion rates, a linear relationship between erosion rate and surface concentration results for all plausible depth settings. At low depths and shallow adsorption, this linear range extends to 0.1mm ky^{-1}, while in typical tropical settings where soils are deep and Be penetrates deeply, the lowest possible erosion rate measurable is ca. 10 mm ky^{-1}.
b.) Integration time scale of erosion rates is calculated (as in the in situ approach) by dividing the adsorption depth 1/k by the erosion rate.

Table 1: Measured fluxes of ^{10}Be and their predicted fluxes from independent measurements. Calculations are the average modeled fluxes of Heikkilä (2007) and Field et al. (2006) for long-term solar activity and geomagnetic fields.

type	**lat**	**lon**	**alt.**	**age**	**^{10}Be flux calculated from data**	**reference**	**flux from average modeled**
	deg	*deg*	*m*	*y BP*	*10^5 atom cm^{-2} yr^{-1}*		*10^5 atom cm^{-2} yr^{-1}*
Maar	-37	-12	200	0.4-2ka	9.9	Ljung et al., 2007	7
Lake	32	35	950	0-60 ka	7.5	Belmaker et al., 2008	6
Loess	35	109	1500	0-80ka	n.a.	Zhou et al., 2007	8
Ice Core	72	-38	3200	0-9 ka	3.0	Vonmoos et al., 2006	3
Rainfall	28	130	5	Modern	28	Maejima et al., 2005	16
Rainfall	28	130	200	Modern	25	Maejima et al., 2005	16
Rainfall	-41	178	10	Modern	10.2	Graham et al., 2003	14
Rainfall	11	-62	10	Modern	4.0	Brown et al., 1992	3
Rainfall	46	8	440	Modern	7.3	Heikkilä et al., 2008	10
Rainfall	47	8	3580	Modern	8.8	Heikkilä et al., 2008	10

Table 2: Measured inventories of ^{10}Be and their predicted ages from independent terrace and soil ages. This comparison does not take into consideration ^{10}Be inherited during sediment deposition – even for marine deposits with high initial concentrations and does not consider erosion of the surface. We use a decay constant of $5x10^{-7}$ y^{-1} to calculate the expected ^{10}Be and the meteoric flux predicted by Field et al. (2006) and Heikkilä (2007). In some cases, the inventory is a minimum because the lower section of the sampled profile did not have a zero ^{10}Be concentration.

Site	**Age**	**Measured ^{10}Be** *atoms cm^{-2}*	**Expected ^{10}Be** *atoms cm^{-2}*	**Reference**
Virginia Piedmont	~10 My	1.1×10^{12}	2.5×10^{12}	Pavich et al. 1985
	~3 My	2.8×10^{11}	2.0×10^{12}	Pavich et al. 1984
	~1.5-0.7 My	2.2×10^{11}	1.3×10^{12}	Pavich et al. 1984
	~180 ky	$7.8x\ 10^{10}$	2.2×10^{11}	Pavich et al. 1984
	~180 ky	$5.9x\ 10^{10}$	2.2×10^{11}	Pavich et al. 1984
Yugoslavia	recent	$>1.8 \times 10^{11}$	---	Pavich and Vidic, 1993
South Mali Ferricrete	Quaternary	1.2×10^{11}	1.3×10^{12}	Barg et al. 1997
Merced R., California	recent	$> 5.3 \times 10^{11}$	---	Pavich et al. 1986
	recent	$> 5.9 \times 10^{11}$	---	Pavich et al. 1986
Australian soils	>2 My	$> 5 \times 10^{11}$	---	Balco, 2004
Salisbury, Minnesota soil	15 ky	$1.9x\ 10^{10}$	$1.8\text{-}2.0 \times 10^{10}$	Balco, 2004
Kikai Is.raised coral terrace	125-120 ky	2.75×10^{11}	2.2×10^{11}	Maejiima et al., 2005
Kikai Is.raised coral terrace	100-95 ky	3.63×10^{11}	4.9×10^{11}	Maejiima et al., 2005
Kikai Is.raised coral terrace	80-70 ky	3.4×10^{11}	5.3×10^{11}	Maejiima et al., 2005
Kikai Is.raised coral terrace	60-50 ky	1.53×10^{11}	1.5×10^{11}	Maejiima et al., 2005
Kikai Is.raised coral terrace	45-35 ky	5.1×10^{10}	2.5×10^{10}	Maejiima et al., 2005
Kikai Is.raised coral terrace	3.9-3.5 ky	2.2×10^{10}	2.2×10^{10}	Maejiima et al., 2005